Folate-Guided Protein Degradation by Immunomodulatory Imide Drug-Based Molecular Glues and Proteolysis Targeting Chimeras

He Chen,[#] Jing Liu,[#] H. Ümit Kaniskan, Wenyi Wei,* and Jian Jin*

Read Online

ACCESS | Metrics & More | Article Recommendations | SI Supporting Information

ABSTRACT: Molecular glues and proteolysis targeting chimeras (PROTACs) are promising new therapeutic modalities. However, the lack of specificity for molecular glue- or PROTAC-mediated proteolysis in cancer cells versus normal cells raises potential toxicity concerns that will likely limit their clinical applications. Here, we developed a general strategy to deliver immunomodulatory imide drug (IMiD)-based molecular glues and PROTACs to folate receptor α (FOLR1)-positive cancer cells. Specifically, we designed a folate-caged pomalidomide prodrug, FA-S2-POMA, by incorporating a folate group as a caging and guiding element and validated its degradation effect on its neo-substrates in FOLR1-positive cancer cells in a FOLR1-dependent manner. We also developed a folate-caged pomalidomide-based anaplastic lymphoma kinase (ALK) PROTAC, FA-S2-MS4048, which effectively degraded ALK fusion proteins in cancer cells, again in a FOLR1-dependent manner. This novel approach provides a generalizable platform for the targeted delivery of IMiD-based molecular glues and PROTACs to FOLR1-expressing cancer cells with the potential to ameliorate toxicity.
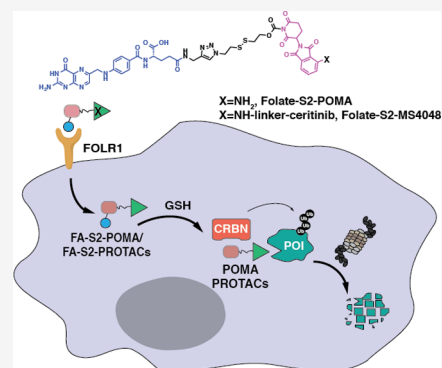
INTRODUCTION

Molecular glues are small molecules that bind E3 ligases and induce new protein−protein interactions between the E3 ligases and previously unrelated proteins in the native cellular environment (termed as neo-substrates), resulting in poly-ubiquitination and subsequent degradation of the neo-substrates by the ubiquitin-proteasome system (UPS).[1] Several classes of molecular glues have been reported, which include immunomodulatory imide drugs (IMiDs),[2−4] sulfonamides,[5,6] and cyclin K degraders.[7−9] Among them, IMiDs such as thalidomide, pomalidomide, and lenalidomide are the most well-studied molecular glues, which recruit the endogenous cereblon (CRBN) E3 ubiquitin ligase[2] and degrade several intracellular protein targets, such as IKZFs,[3,4] CK1α,[10] GSPT1,[11] SALL4,[12] p63,[13] and ARID2.[14] In addition to molecular glues, proteolysis targeting chimeras (PROTACs), which are heterobifunctional small molecules with one moiety binding E3 ligases and another moiety binding target proteins, have emerged as a new class of promising therapeutic modalities.[1,15−18] IMiDs as ligands of the E3 ligase CRBN have been widely used to develop effective PROTACs since 2015.[19,20] Multiple IMiDs have been used in the clinic for treating cancer,[1] and a number of IMiD-based PROTACs are in clinical development as anticancer therapeutics.[21,22]

However, molecular glues and PROTACs have potential toxicity as they may degrade the protein targets in normal, noncancerous tissues in addition to cancer cells. Notably, thalidomide, which was approved in the late 1950s for treating morning sickness in pregnant women in Europe, was banned

soon after the discovery that it caused widespread severe birth defects.[23] It was recently uncovered that the teratogenic effects of thalidomide are likely due to the degradation of CRBN neo-substrates p63[13] and SALL4[12] by thalidomide. Degradation of CRBN neo-substrates such as GSPT1 by IMiD-based PROTACs has also been reported.[21,24] These potential toxicity concerns may limit utilities of molecular glues and PROTACs in the clinic. Therefore, it is critical to develop a cancer-cell-targeted delivery system for molecular glues and PROTACs to reduce potential toxicity and increase the therapeutic window. While the antibody drug-conjugate (ADC) approach has been used for delivering PROTACs in several proof-of-concept studies,[25−29] none of the antibody-based PROTACs have been advanced to clinic development.

Folate conjugation is one of the best-established methods for targeted delivery of drugs to cancer cells because folate receptor α (FOLR1) is highly expressed in many human cancers, including multiple myeloma (MM), lymphoma, and nonsmall cell lung cancer (NSCLC), while normal tissues exhibit relatively low FOLR1 expression.[30] In addition to FOLR1, other receptors and transporters of folate, such as
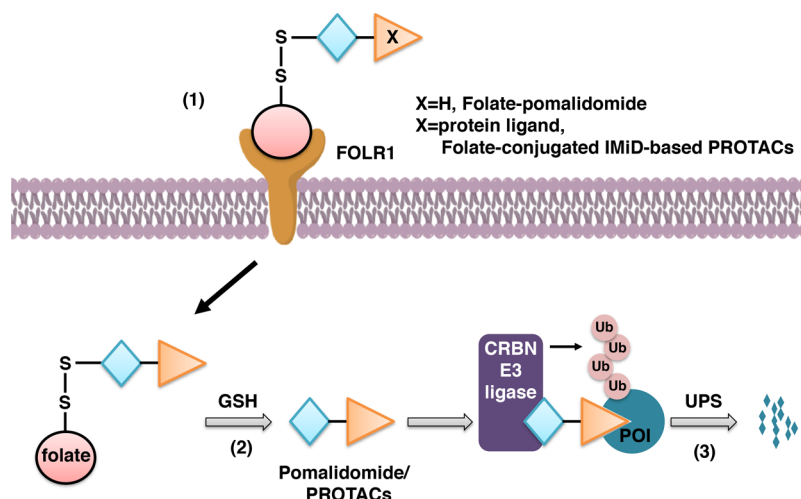
Figure 1. Schematic diagram showing the mode of action of folate-pomalidomide and folate-conjugated IMiD-based PROTACs. Upon binding FOLR1 on the cell membrane (1), folate-pomalidomide or folate-conjugated IMiD-based PROTACs are transported into cells, and the active pomalidomide or PROTACs are released after the reduction by endogenous GSH (2). The active pomalidomide or PROTACs recruit endogenous CRBN E3 ligase, leading to polyubiquitination and subsequent degradation of IKZFs or the proteins of interest (POIs) by the UPS (3).
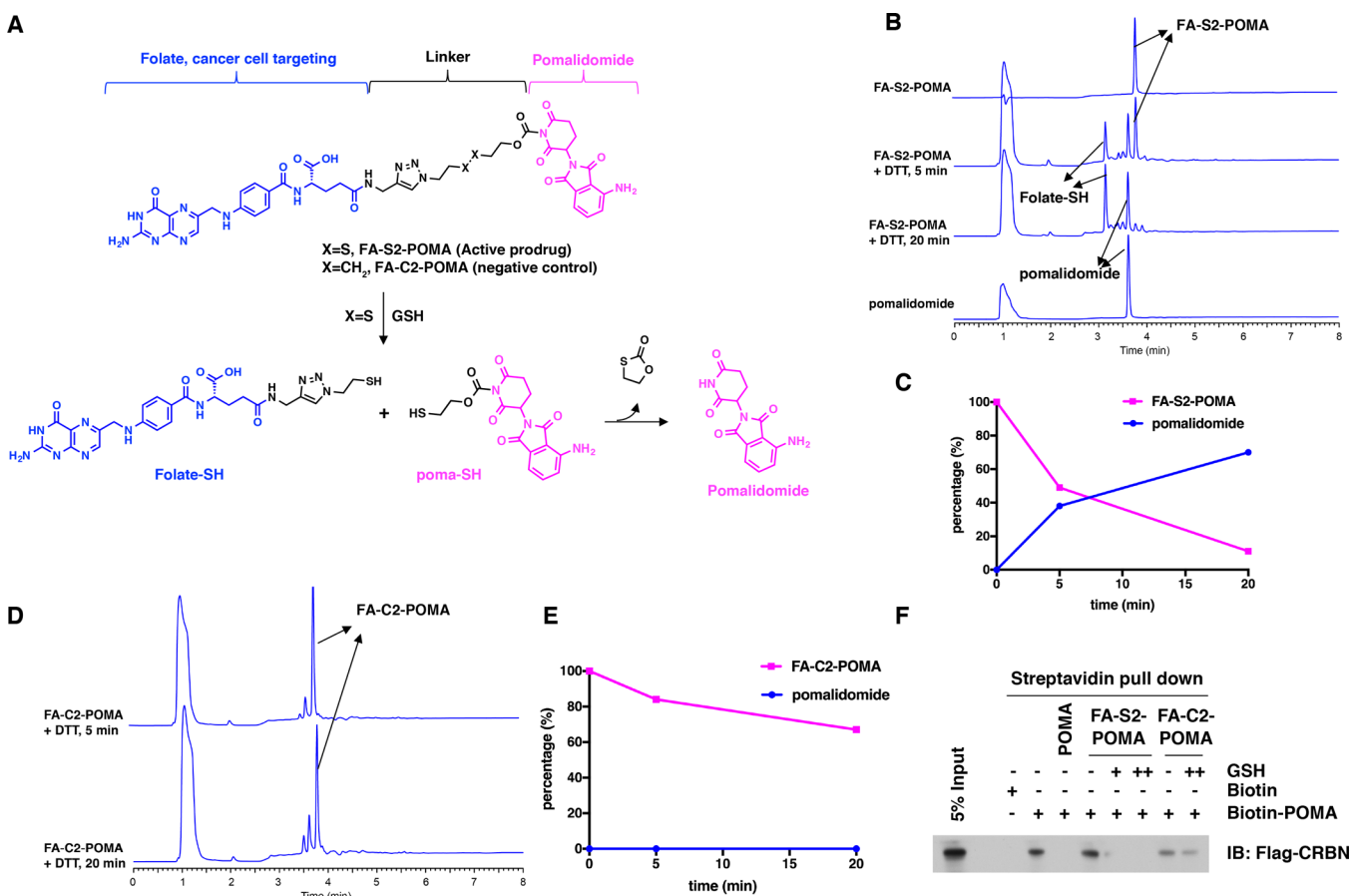

Figure 2. Release of pomalidomide from FA-S2-POMA *in vitro*. (A) Schematic diagram showing chemical structures of folate-S2-pomalidomide (FA-S2-POMA) and its negative control (folate-C2-pomalidomide, FA-C2-POMA), as well as the release of pomalidomide from FA-S2-POMA. FA-S2-POMA is cleaved after reduction by GSH, releasing a folate derivate (folate-SH) and pomalidomide derivate (poma-SH), which then releases pomalidomide and 1,3-oxathiolan-2-one via spontaneous intramolecular cyclization. (B, C) HPLC analysis of folate-S2-pomalidomide (FA-S2-POMA) after incubation with DTT (2 equiv) at 37 °C in PBS for 5 and 20 min. (D, E) HPLC analysis of folate-C2-pomalidomide (FA-C2-POMA) after incubation with DTT (2 equiv) at 37 °C in PBS for 5 and 20 min. (F) Reduction of FA-S2-POMA with GSH leads to the release of pomalidomide, which competes with biotinylated pomalidomide (biotin-POMA) for binding with flag-tagged CRBN (flag-CRBN). Cell lysates derived from HEK293T cells were incubated with biotin or biotin-POMA, with or without pomalidomide, FA-S2-POMA or FA-C2-POMA for 1 h, and with or without pretreatment with GSH (+: 1 mM, ++: 5 mM).

Scheme 1. Synthesis of FA-S2-POMA and FA-C2-POMA[a]
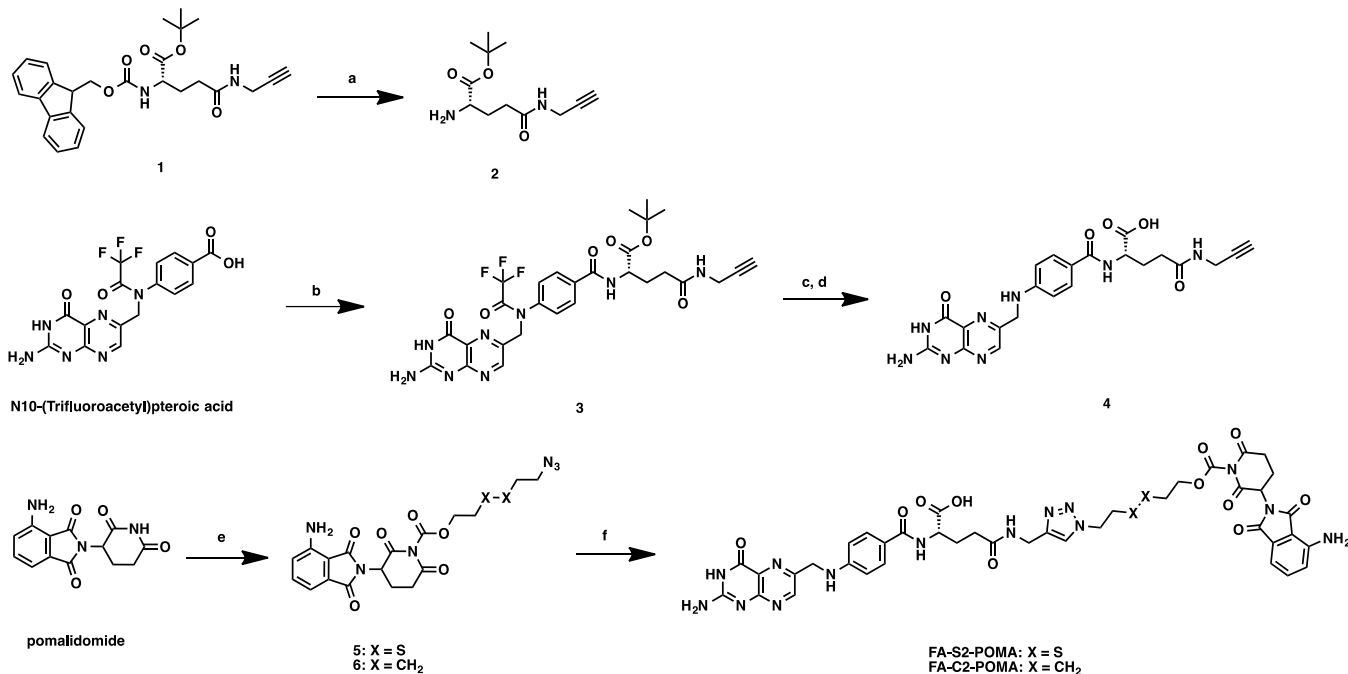
[a]Reaction conditions: (a) dimethylamine, DMF, rt., 30 min; (b) **2**, EDCI, HOAt, NMM, DMSO, rt., 1 h; (c) TFA/CH₂Cl₂, rt., 2 h; (d) K₂CO₃, MeOH/H₂O, rt., 1 h; (e) 2-((2-azidoethyl)disulfanyl)ethyl carbonochloridate for compound **5** (6-azidohexyl carbonochloridate for compound **6**), NaH, DMF, rt., 2 h; and (f) **4**, CuSO₄·5H₂O, sodium ascorbate, DMF/H₂O, 50 °C, 2 h.

FOLR2/3, the reduced folate carrier SLC19A1, and the proton-coupled folate transporter SLC46A1, are known, but with relatively low binding affinity to folate.[30,31] Notably, multiple MM patients have relatively high levels of FOLR1 on the membrane of plasma cells and the expanded cancer cells, compared with healthy individuals.[32] Furthermore, MM patients usually have folate deficiency, which in turn stimulates the expression of FOLR1.[33,34] These findings suggest that folate-conjugated molecular glues and PROTACs might be selective for MM and other cancer cells with high FOLR1 expression.

Very recently, we developed a cancer cell-selective delivery strategy for PROTACs that recruit the von Hippel–Lindau (VHL) E3 ubiquitin ligase by conjugating a folate group to the hydroxyl group of the VHL ligand.[35] However, a targeted delivery strategy for molecular glues or IMiD-based PROTACs has not been reported. Herein, we report the development of a folate conjugation approach as a generalizable platform for selectively delivering IMiD-based molecular glues and PROTACs to cancer cells with high FOLR1 expression. We designed a folate-caged pomalidomide prodrug, FA-S2-POMA, featuring a reduction-cleavable disulfide linker (Figure 1). We show that FA-S2-POMA can be reduced by intracellular glutathione (GSH) to release active pomalidomide and degrade its CRBN neo-substrates IKZFs in cancer cells with high FOLR1 expression, but not in cells with no FOLR1 expression. We also designed a folate-caged pomalidomide-based anaplastic lymphoma kinase (ALK) PROTAC, FA-S2-MS4048, and validated its degradation of ALK fusion proteins in cancer cells in a FOLR1-dependent manner. Our results suggest that this folate-caging strategy can be a general approach to the targeted delivery of IMiD-based molecular glues and PROTACs to cancer cells with a high FOLR1 expression.

■ RESULTS AND DISCUSSION

Design and Synthesis of FA-S2-POMA. Given that pomalidomide, an IMiD-based molecular glue, has been used in the clinic and has been widely utilized as a CRBN-recruiting ligand for developing PROTACs, we chose it as an example to assess the feasibility of our folate conjugation strategy. Specifically, we incorporated a folate group onto the glutarimide N–H group of pomalidomide for cancer-cell-specific drug delivery (Figure 1). Because the glutarimide N–H group of pomalidomide is pivotal for binding the CRBN E3 ubiquitin ligase,[36] and the caging at this position blocks its interaction with CRBN, as shown in the previous studies by us and others,[19,37,38] we expect the folate-caged pomalidomide, FA-S2-POMA (Figure 2A), to be inert and incapable of degrading proteins. To release pomalidomide after its entry into cancer cells guided by the folate group, pomalidomide and folic acid were conjugated via a reduction-cleavable disulfide bond (−S−S−) (Figure 2A), which can be cleaved by endogenous GSH in cells, followed by spontaneous intra-molecular cyclization to release the active pomalidomide and 1,3-oxathiolan-2-one (Figure 2A).[39] Given that GSH levels are relatively low in the blood or extracellular matrix[40] but high in the cytoplasm,[41] it is highly likely that FA-S2-POMA could remain in the −S−S− state before it enters the cells and is subsequently cleaved by GSH. To obtain a noncleavable, negative control of FA-S2-POMA, the disulfide bond was replaced by a carbon−carbon bond to give FA-C2-POMA (Figure 2A), which cannot be easily cleaved by GSH and thus will likely remain caged after entering the cells. The synthesis of FA-S2-POMA and FA-C2-POMA is outlined in Scheme 1. An amide coupling reaction of commercially available N10-(trifluoroacetyl)pteroic acid with intermediate **2**, which was obtained from the deprotection of compound **1** with dimethylamine, produced intermediate **3**. The deprotection
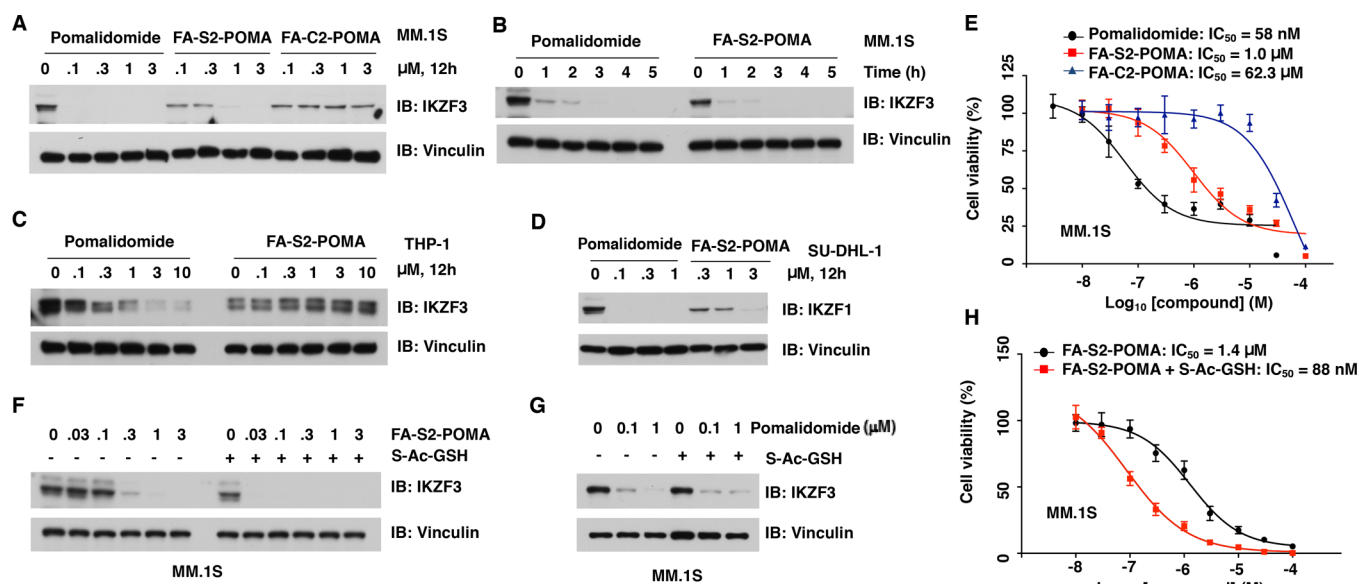
Figure 3. FA-S2-POMA degrades IKZFs in FOLR1-positive cancer cells in a concentration- and time-dependent manner. (A) Western blotting of IKZF3 in MM.1S cells treated with indicated concentrations of pomalidomide, FA-S2-POMA, or FA-C2-POMA for 12 h. (B) Western blotting of IKZF3 in MM.1S cells treated with 0.1 μM of pomalidomide or 1 μM of FA-S2-POMA for indicated times. (C) Western blotting of IKZF3 in THP-1 cells treated with indicated concentrations of pomalidomide or FA-S2-POMA for 12 h. (D) Western blotting of IKZF1 in SU-DHL-1 cells treated with indicated concentrations of pomalidomide or FA-S2-POMA for 12 h. (E) Cell viability of MM.1S cells after being treated with indicated concentrations of pomalidomide, FA-S2-POMA, or FA-C2-POMA for 72 h. (F, G) Western blotting of IKZF3 in MM.1S cells treated with indicated concentrations of FA-S2-POMA (F) or pomalidomide (G) for 12 h, with or without pretreatment with S-Ac-GSH (1 mM) for 12 h. (H) Cell viability of MM.1S cells after being treated with indicated concentrations of FA-S2-POMA for 72 h, with or without pretreatment with S-Ac-GSH (1 mM) for 12 h.

of the *tert*-butyl ester of intermediate **3** with trifluoroacetic acid, followed by basic hydrolysis of the trifluoroacetamide group, afforded the alkyne-containing folic acid **4**,[35] which was used for the following copper-catalyzed azide-alkyne cycloaddition reaction (CuAAC). The condensation reaction of pomalidomide and 2-((2-azidoethyl)disulfanyl)ethyl carbonochloridate, followed by CuAAC reaction with **4**, resulted in the desired compound FA-S2-POMA. The negative control, FA-C2-POMA, was synthesized using the same synthetic route, with 6-azidohexyl carbonochloridate instead of 2-((2-azidoethyl)disulfanyl)ethyl carbonochloridate as a starting material.

***In Vitro* Release of Pomalidomide from FA-S2-POMA.** To determine whether pomalidomide can be released from this folate-pomalidomide conjugate, FA-S2-POMA and its negative control, FA-C2-POMA, were incubated with dithiothreitol (DTT) under physiological conditions [37 °C, in phosphate-buffered saline (PBS)] and then subjected to high-performance liquid chromatography (HPLC) analysis. Notably, the addition of DTT led to the efficient release of pomalidomide from FA-S2-POMA, but not from FA-C2-POMA (Figure 2B−E). Furthermore, while FA-S2-POMA and FA-C2-POMA in the caged, inert form do not compete with biotinylated-pomalidomide to bind the CRBN E3 ubiquitin ligase, pretreatment of FA-S2-POMA, but not FA-C2-POMA, with GSH led to the release of pomalidomide, which effectively competes with biotinylated pomalidomide for binding CRBN E3 ubiquitin ligase (Figure 2F). These results suggest that FA-S2-POMA as a folate-caged pomalidomide prodrug can release pomalidomide, the active drug, upon the treatment with a reducing agent such as GSH under physiological conditions.

FA-S2-POMA Degrades IKZFs in FOLR1-Positive Cancer Cells in a Concentration- and Time-Dependent

Manner. We next aimed at showing that the folate group can effectively guide and deliver folate-caged pomalidomide into cells that express FOLR1, but not cells with no FOLR1 expression, resulting in effective degradation of the pomalidomide-CRBN neo-substrates IKZF3 and IKZF1. To this end, we compared the effect of free pomalidomide, FA-S2-POMA, and FA-C2-POMA on the multiple myeloma cell line MM.1S and lymphoma cell line SU-DHL-1 that express FOLR1, as well as the myeloid leukemia cell line THP-1 that does not express FOLR1 (Figure S1A). Notably, pomalidomide degraded IKZF3 or IKZF1 in all three cell lines in a concentration- and time-dependent manner [Figure 3A−C (IKZF3 in MM.1S and THP-1 cells) and 3D (IKZF1 in SU-DHL-1 cells)]. On the other hand, FA-S2-POMA degraded IKZF3 or IKZF1 in FOLR1-postive MM.1S (Figure 3A,B, IKZF3) and SU-DHL-1 cells (Figure 3D, IKZF1), but not in FOLR1-negative THP-1 cells (Figure 3C, IKZF3). These results suggest that FA-S2-POMA selectively targets FOLR1-expressing cells over FOLR1-negative cells. Moreover, the noncleavable negative control FA-C2-POMA was ineffective in degrading IKZF3 in MM.1S cells (Figure 3A) likely due to its inability to undergo the uncaging process.

Next, we studied the antiproliferation effect of FA-S2-POMA in MM.1S cells and found that FA-S2-POMA effectively inhibited the proliferation of MM.1S cells with an IC$_{50}$ of 1.0 μM, which is more potent than FA-C2-POMA (IC$_{50}$ = 62.3 μM) but less potent than pomalidomide (IC$_{50}$ = 58 nM) (Figure 3E), suggesting that the uncaging process is likely pivotal for the effectiveness of FA-S2-POMA. The antiproliferation effect of these compounds is consistent with their effect on degrading IKZF3 in MM.1S cells (Figure 3A). Moreover, folate-SH (FA-SH, Scheme S1), which is the major byproduct released after the disulfide bond is reduced by GSH,
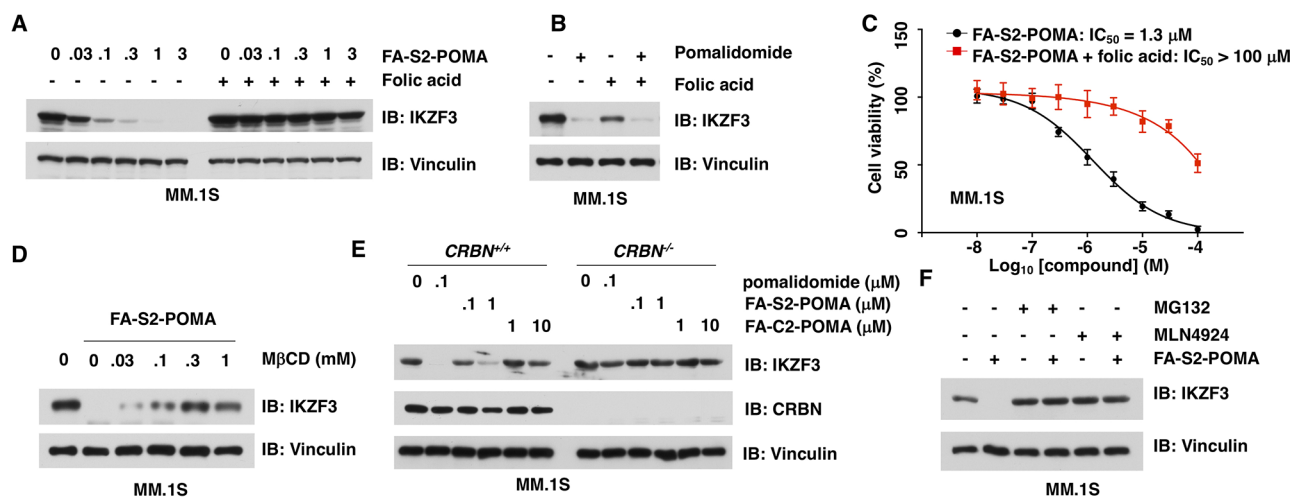
Figure 4. FA-S2-POMA degrades IKZF3 in a FOLR1-, CRBN-, and proteasome-dependent manner. (A, B) Western blotting of IKZF3 in MM.1S cells treated with indicated concentrations of FA-S2-POMA (A) or pomalidomide (0.1 μM) (B), with or without the presence of 2.5 mM folic acid. (C) Cell viability of MM.1S cells after being treated with indicated concentrations of FA-S2-POMA for 72 h, with or without the presence of 2.5 mM folic acid. (D) Western blotting of IKZF3 in MM.1S cells treated with indicated concentration of the endocytosis inhibitor MβCD for 12 h, followed by the treatment with 1 μM of FA-S2-POMA for another 12 h. (E) Western blotting of IKZF3 in MM.1S-CRBN-WT or MM.1S-CRBN-KO cells treated with indicated concentrations of pomalidomide, FA-S2-POMA, or FA-C2-POMA for 12 h. (F) Western blotting of IKZF3 in MM.1S cells treated with 1 μM of FA-S2-POMA for 12 h, with or without the presence of 10 μM MG132 or 1 μM MLN4924.
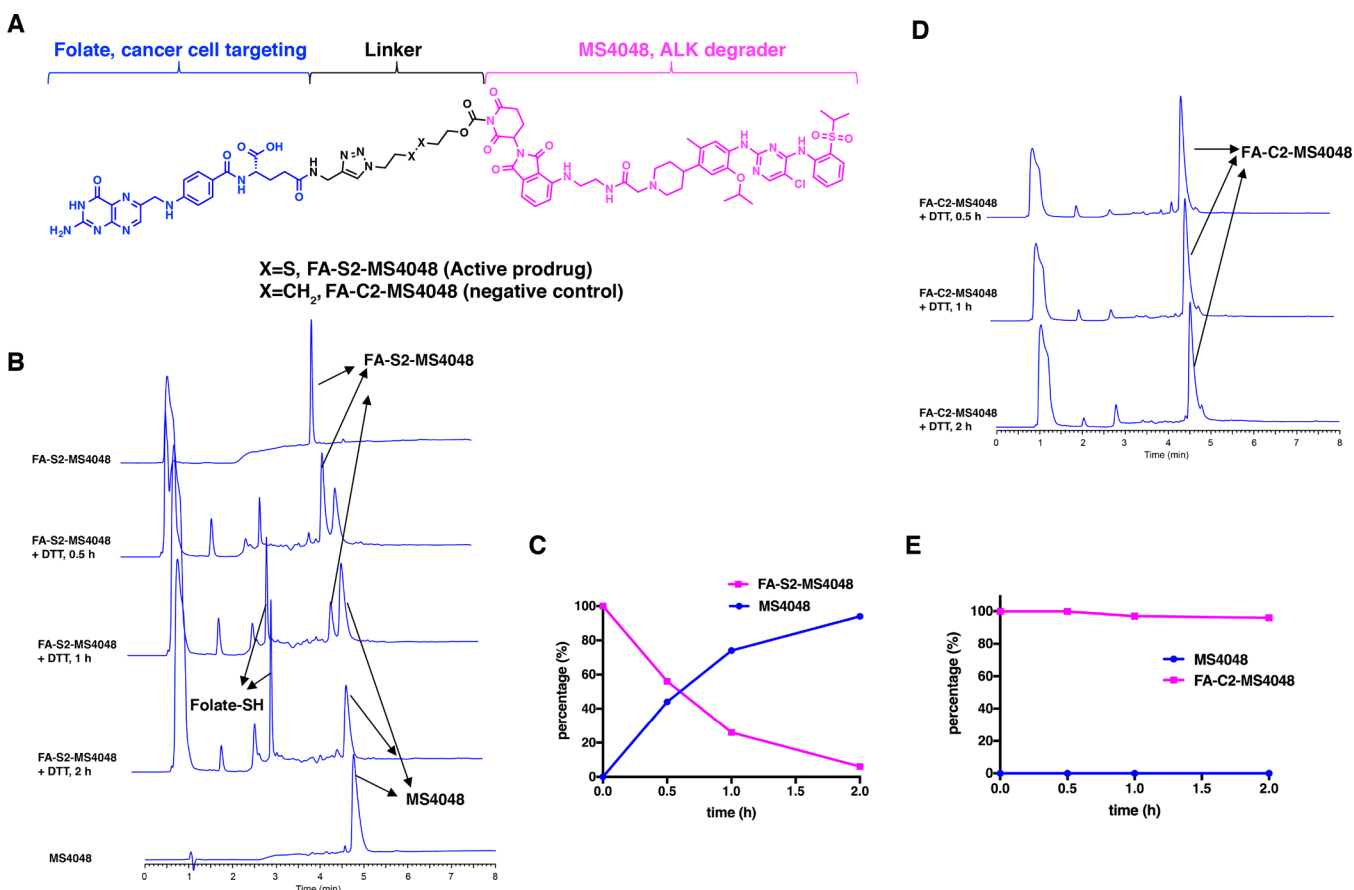

Figure 5. Release of MS4048 from FA-S2-MS4048 but not from FA-C2-MS4048 *in vitro*. (A) Chemical structures of FA-S2-MS4048 and its negative control, FA-C2-MS4048. (B, C) HPLC analysis of FA-S2-MS4048 after incubation with DTT (10 equiv) at 37 °C in PBS for 0.5, 1, and 2 h. (D, E) HPLC analysis of FA-C2-MS4048 after incubation with DTT (10 equiv) at 37 °C in PBS for 0.5, 1, and 2 h.

as well as folic acid itself, did not inhibit the proliferation in MM.1S and SU-DHL-1 cells (Figure S1B,C). This result suggests that the antiproliferation effect of FA-S2-POMA is not

due to the folate adduct released from the reduction of the disulfide bond by GSH. We also treated MM.1S cells with S-acetyl-L-glutathione (S-Ac-GSH), which is stable under

Scheme 2. Synthesis of FA-S2-MS4048 and FA-C2-MS4048[a]
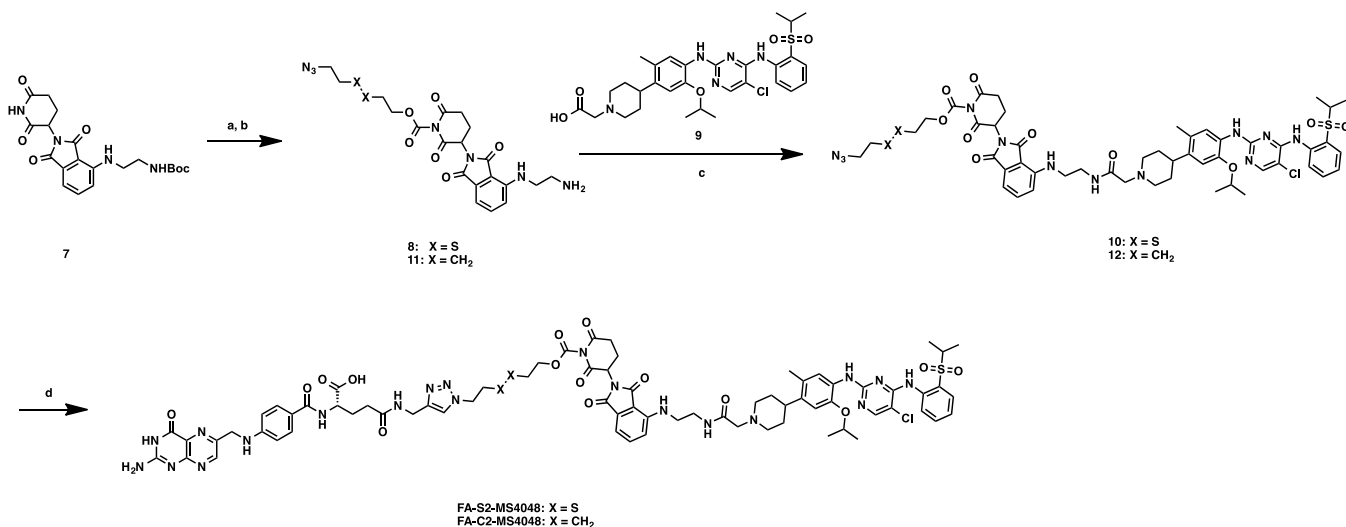
[a]Reaction conditions: (a) 2-((2-azidoethyl)disulfanyl)ethyl carbonochloridate for compound **8** (6-azidohexyl carbonochloridate, for compound **11**), NaH, DMF, rt., 1 h; (b) TFA/CH$_2$Cl$_2$, rt., 1 h; (c) 2-(4-(4-((5-chloro-4-((2-(isopropylsulfonyl)phenyl)-amino)pyrimidin-2-yl)amino)-5-isopropoxy-2-methylphenyl)piperidin-1-yl)acetic acid (compound **9**), EDCI, HOAt, NMM, DMSO, rt., 4 h; (d) **4**, CuSO$_4$·5H$_2$O, sodium ascorbate, DMF/H$_2$O, 50 °C, 2 h.

physiological conditions and can be directly taken up by cells and converted into GSH by intracellular thioesterases to increase the intracellular levels of GSH.[42,43] As expected, pretreatment with S-Ac-GSH significantly increased the potency of FA-S2-POMA (Figure 3F), but not pomalidomide (Figure 3G), in degrading IKZF3 in MM.1S cells. Consistent with these results, pretreatment with S-Ac-GSH significantly increased the potency of FA-S2-POMA in inhibiting the proliferation of MM.1S cells (Figure 3H) to a comparable level displayed by pomalidomide. These data further support that after folate-guided cellular uptake, FA-S2-POMA is cleaved by intracellular GSH, leading to the release of pomalidomide, which, in turn, degrades pomalidomide-CRBN neo-substrates and suppresses cancer cell proliferation.

FA-S2-POMA Degrades IKZF3 in a FOLR1-, CRBN- and Proteasome-Dependent Manner. To assess the dependence of the folate-caged pomalidomide prodrug on FOLR1 expression, MM.1S cells were cotreated with FA-S2-POMA and 2.5 mM folic acid to saturate FOLR1 binding. Notably, folic acid effectively antagonized the effect of FA-S2-POMA (Figure 4A), but not pomalidomide (Figure 4B), on degrading IKZF3 in MM.1S cells. Consistent with this result, cotreatment with folic acid led to a significant reduction in the potency of FA-S2-POMA in suppressing the proliferation of MM.1S cells (Figure 4C). Similarly, cotreatment with the endocytosis inhibitor MβCD[44] compromised the effect of FA-S2-POMA on degrading IKZF3 in this experimental setting (Figure 4D). Collectively, these results suggest that FOLR1 and subsequent endocytosis are important for FA-S2-POMA entering the cells. Furthermore, depletion of the endogenous *CRBN* E3 ubiquitin ligase completely abolished the effect of pomalidomide and FA-S2-POMA on degrading IKZF3 in MM.1S cells (Figure 4E, Figure S1D−F), indicating that the IKZF3 degradation effect of FA-S2-POMA depends on the CRBN E3 ubiquitin ligase. Finally, we also treated MM.1S cells with FA-S2-POMA with or without the proteasome inhibitor MG132[45] or the cullin-RING E3 ligase (CRL) neddylation inhibitor MLN4924[46] and found that both inhibitors totally blocked the effect of FA-S2-

POMA on degrading IKZF3 (Figure 4F). Taken together, these results suggest that FA-S2-POMA induces the degradation of IKZF3 in a FORL1-, CRBN- and proteasome-dependent manner.

Design and Synthesis of FA-S2-MS4048. With the goal of expanding utilities of this folate-caging strategy, we next turned our attention to CRBN-recruiting PROTACs, as IMiDs such as pomalidomide have been widely used as a CRBN ligand for various PROTACs.[19,20,47] ALK mutation is a driver event for many types of human cancers, including anaplastic large cell lymphomas (ALCL)[48] and nonsmall-cell lung cancer (NSCLC).[49] We previously developed an IMiD-based ALK PROTAC, MS4048, which potently degrades ALK fusion proteins.[38] Thus, based on MS4048, we designed and synthesized a folate-caged PROTAC, FA-S2-MS4048, and its negative control FA-C2-MS4048 and assessed their effects on degrading ALK fusion proteins in cancer cells. FA-S2-MS4048 and FA-C2-MS4048 share the same design as FA-S2-POMA and FA-C2-POMA, featuring the disulfide and carbon−carbon bonds, respectively (Figure 5A). The synthesis of FA-S2-MS4048 and FA-C2-MS4048 is outlined in Scheme 2. Condensation reaction of compound **7** and 2-((2-azidoethyl)-disulfanyl)ethyl carbonochloridate, followed by deprotection of the Boc group, afforded intermediate **8**. The subsequent amide coupling reaction of intermediate **8** with compound **9**, followed by CuAAC reaction with intermediate **4**, provided the desired compound FA-S2-MS4048. FA-C2-MS4048 was prepared using the same procedures with 6-azidohexyl carbonochloridate as a starting material, instead of 2-((2-azidoethyl)disulfanyl)ethyl carbonochloridate.

***In Vitro* Release of MS4048 from FA-S2-MS4048.** First, we evaluated the release of MS4048 from FA-S2-MS4048 and its negative control FA-C2-MS4048 by incubating them with DTT at 37 °C in PBS and found that the DTT treatment led to efficient release of MS4048 from FA-S2-MS4048 (Figure 5B,C), but not from FA-C2-MS4048 (Figure 5D,E). Compared to FA-S2-POMA, the reduction rate of FA-S2-
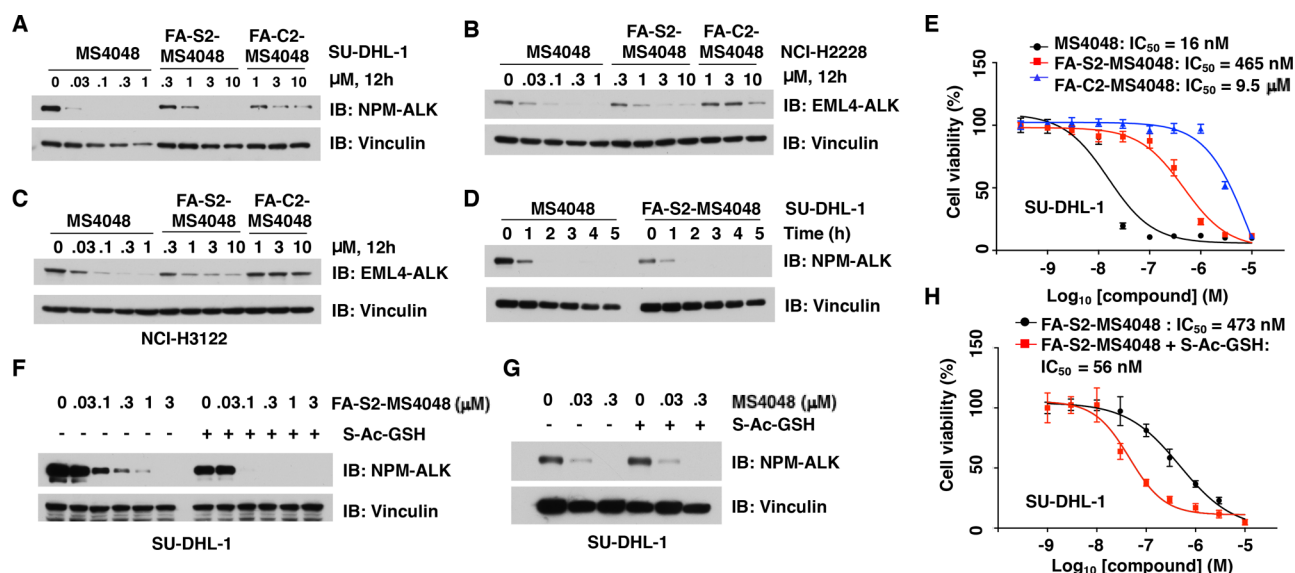
Figure 6. FA-S2-MS4048 degrades ALK fusion proteins in a concentration- and time-dependent manner. (A) Western blotting of NPM-ALK in SU-DHL-1 cells treated with indicated concentrations of MS4048, FA-S2-MS4048, or FA-C2-MS4048 for 12 h. (B, C) Western blotting of EML4-ALK fusion protein in two NSCLC cell lines, NCI-H2228 and NCI-H3122, treated with indicated concentrations of MS4048, FA-S2-MS4048, or FA-C2-MS4048 for 12 h. (D) Western blotting of NPM-ALK in SU-DHL-1 cells treated with 0.3 μM MS4048 or 3 μM FA-S2-MS4048 for indicated times. (E) Cell viability of SU-DHL-1 cells after being treated with indicated concentrations of MS4048, FA-S2-MS4048, or FA-C2-MS4048 for 72 h. (F, G) Western blotting of NPM-ALK in SU-DHL-1 cells treated with indicated concentrations of FA-S2-MS4048 or MS4048 for 12 h, with or without pretreatment with S-Ac-GSH (1 mM) for 12 h. (H) Cell viability of SU-DHL-1 cells after being treated with indicated concentrations of FA-S2-MS4048 for 72 h, with or without pretreatment with S-Ac-GSH (1 mM) for 12 h.
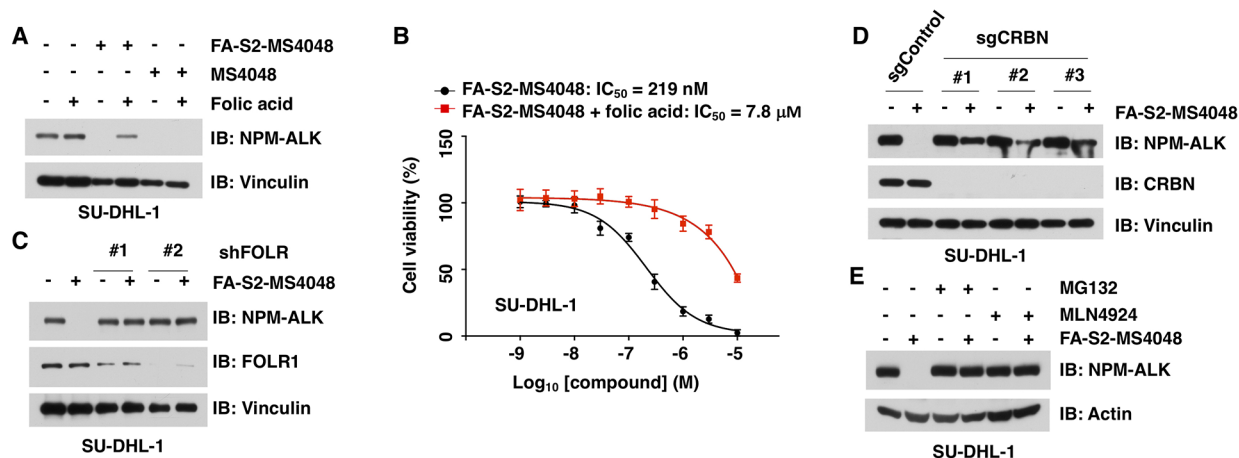

Figure 7. FA-S2-MS4048 degrades the NPM-ALK fusion protein in a FOLR1-, CRBN- and proteasome-dependent manner. (A) Western blotting of NPM-ALK in SU-DHL-1 cells treated with MS4048 (0.3 μM) or FA-S2-MS4048 (3 μM), with or without the presence of 2.5 mM of folic acid. (B) Cell viability of SU-DHL-1 cells after being treated with indicated concentrations of FA-S2-MS4048 for 72 h, with or without the presence of 2.5 mM folic acid. (C) Western blotting of NPM-ALK in SU-DHL-1 cells with knockdown of *FOLR1* and treated with FA-S2-MS4048 (3 μM) for 12 h. (D) Western blotting of NPM-ALK in SU-DHL-1 cells with *CRBN*-WT or *CRBN*-KO cells and treated with FA-S2-MS4048 (3 μM) for 12 h. (E) Western blotting of NPM-ALK in SU-DHL-1 cells treated with 3 μM FA-S2-MS4048 for 12 h, with or without the presence of 10 μM MG132 or 1 μM MLN4924.

MS4048 is lower (Figure 5B,C). It is unclear what contributes to the lower release rate.

FA-S2-MS4048 Degrades ALK Fusion Proteins in a Concentration- and Time-Dependent Manner. Next, we assessed the effect of FA-S2-MS4048 in SU-DHL-1 cells, an ALCL cell line harboring the NPM-ALK fusion protein,[48] as well as NCI-H2228 and NCI-H3122 cells, two NSCLC cell lines, with the EML4-ALK fusion protein.[49] Notably, FA-S2-MS4048 effectively degraded NPM-ALK in SU-DHL-1 cells (Figure 6A) and EML4-ALK in NCI-H2228 and NCI-H3122 cells (Figure 6B,C, Figure S2A,B) in a concentration-

dependent manner. While FA-S2-MS4048 is less potent than MS4048, it is more potent than FA-C2-MS4048 in degrading these ALK proteins (Figure 6A−C, Figure S2A,B). It is unclear why FA-C2-MS4048 has some degradation effect, in particular, in SU-DHL-1 cells. A possible explanation is that the carbamate group in FA-C2-MS4048 could be hydrolyzed to release MS4048, and the rate of hydrolysis is dependent on the cellular context. We next determined that FA-S2-MS4048 degraded NPM-ALK in SU-DHL-1 cells in a time-dependent manner (Figure 6D). Significant degradation was observed as early as 1 h. We also found that FA-S2-MS4048 effectively

12279

inhibited the proliferation of SU-DHL-1 cells with an IC_{50} of 465 nM (Figure 6E). It is less potent than MS4048 (IC_{50} = 16 nM) but more potent than FA-C2-MS4048 (IC_{50} = 9.5 μM) (Figure 6E). The antiproliferative effect of FA-S2-MS4048, MS4048, and FA-C2-MS4048 in SU-DHL-1 cells is consistent with their effect on degrading the NPM-ALK fusion protein. In addition, similar to the results obtained for FA-S2-POMA, we found that pretreatment with S-Ac-GSH to supplement the intracellular GSH level led to a significant increase in the potency of FA-S2-MS4048 (Figure 6F, Figure S2C,D), but not MS4048 (Figure 6G), in degrading NPM-ALK in SU-DHL-1 cells and EML4-ALK in NCI-H2228 and NCI-H3122 cells. Furthermore, pretreatment with S-Ac-GSH significantly increased the potency of FA-S2-MS4048 in inhibiting the proliferation of SU-DHL-1 cells (Figure 6H). These data indicate that the intracellular GSH level is important for the effectiveness of FA-S2-MS4048, providing evidence that further supports the proposed mechanism of action.

FA-S2-MS4048 Degrades the NPM-ALK Fusion Protein in a FOLR1-, CRBN- and Proteasome-Dependent Manner. To assess whether FOLR1 is important for the targeted delivery of FA-S2-MS4048, we conducted pretreatment experiments with folic acid and FOLR1 knockdown experiments with shRNAs. First, we found that the pretreatment with folic acid indeed blocked the effect of FA-S2-MS4048, but not of MS4048, on degrading the NPM-ALK fusion protein in SU-DHL-1 cells (Figure 7A). Consistent with this result, the pretreatment with folic acid also significantly reduced the potency of FA-S2-MS4048 in inhibiting the proliferation of SU-DHL-1 cells (Figure 7B). Importantly, the knockdown of *FOLR1* via shRNAs completely abolished the effect of FA-S2-MS4048 on degrading the NPM-ALK fusion protein in SU-DHL-1 cells (Figure 7C). In addition, depletion of the endogenous *CRBN* E3 ligase also significantly reduced the effect of FA-S2-MS4048 on degrading NPM-ALK in SU-DHL-1 cells (Figure 7D). Moreover, inhibition of the proteasome by MG132 or inhibition of CRL neddylation by MLN4924 also blocked the degradation of NPM-ALK in SU-DHL-1 cells (Figure 7E) and EML4-ALK in NCI-H2228 and NCI-H3122 cells (Figure S3A,B). Collectively, these results indicate that the folate-caged pomalidomide-derived ALK PROTAC, FA-S2-MS4048, degrades ALK fusion proteins in cancer cells in a FOLR1-, CRBN-, and proteasome-dependent manner.

CONCLUSIONS

In summary, we developed a folate-caging strategy for targeted delivery of IMiD-based molecular glues and PROTACs to FOLR1-expressing cancer cells. In particular, we designed FA-S2-POMA (a folate-caged pomalidomide prodrug), which features a disulfide bond that can be cleaved by intracellular GSH to release the active molecular glue, pomalidomide. We show that FA-S2-POMA enables targeted delivery of pomalidomide to FOLR1-expressing cancer cells, leading to effective degradation of the CRBN neo-substrates IKZF3 and IKZF1 in a FOLR1-, CRBN- and proteasome-dependent manner. We also developed FA-C2-POMA, a very close analog of FA-S2-POMA with a carbon−carbon bond instead of the disulfide bond, as a control and showed that FA-S2-POMA was indeed more effective than FA-C2-POMA in degrading CRBN neo-substrates and suppressing the proliferation in FOLR1-positive cancer cells. We also found that the treatment of S-Ac-GSH, which increases the intracellular GSH level, significantly

improved the degradation and antiproliferation potencies of FA-S2-POMA. To expand the general applicability of this strategy, we also designed a proof-of-concept folate-caged PROTAC, FA-S2-MS4048, which connects the folate group to the pomalidomide-based ALK PROTAC, MS4048, through the same linker as FA-S2-POMA with a cleavable disulfide bond. We show that this folate-caged IMiD-based PROTAC effectively degraded ALK fusion proteins in FOLR1-expressing cancer cells in a FOLR1-, CRBN- and proteasome-dependent manner. Similarly, FA-S2-MS4048 was more effective than FA-C2-MS4048, a control of FA-S2-MS4048 with a carbon−carbon bond instead of the disulfide bond, in degrading ALK fusion proteins and suppressing the proliferation of cancer cells, and S-Ac-GSH significantly enhanced the degradation and antiproliferation potencies of FA-S2-MS4048. Overall, we provide the scientific community a generalizable platform for the targeted delivery of IMiD-based molecular glues and PROTACs to FOLR1-expressing cancer cells. This novel strategy could circumvent potential toxicity of IMiD-based molecular glues and PROTACs.

EXPERIMENTAL SECTION

Chemistry General Procedures. Common materials or reagents were purchased from commercial sources and used without further purification. Ultraperformance liquid chromatography (UPLC) spectra for compounds were acquired using a Waters Acquity I-Class UPLC system with a photodiode-array detector. Chromatography was performed on a 2.1 Å ∼ 30 mm ACQUITY UPLC BEH C18 1.7 μm column with water containing 3% acetonitrile, 0.1% formic acid as solvent A, and acetonitrile containing 0.1% formic acid as solvent B at a flow rate of 0.8 mL/min. The gradient program was as follows: 1−99% B (1−1.5 min) and 99−1% B (1.5−2.5 min). HPLC spectra were acquired using an Agilent 1200 Series system with a diode array detector for all the intermediates and final products mentioned below. Chromatography was performed on a 2.1 × 150 mm Zorbax 300SB-C18 5 μm column with water containing 0.1% formic acid as solvent A and acetonitrile containing 0.1% formic acid as solvent B at a flow rate of 0.4 mL/min. The gradient program was as follows: 1% B (0−1 min), 1−99% B (1−4 min), and 99% B (4−8 min). High-resolution mass spectrometry (HRMS) data were acquired in positive-ion mode using an Agilent G1969A atmospheric pressure inlet-time-of-flight (API-TOF) spectrometer with an electrospray ionization (ESI) source. Nuclear magnetic resonance (NMR) spectra were acquired on a Bruker DRX-600 spectrometer with 600 MHz for proton (^{1}H NMR) and 151 MHz for carbon (^{13}C NMR); chemical shifts are reported in δ. Preparative HPLC was performed on Agilent Prep 1200 series with a UV detector set to 220 or 254 nm. Samples were injected onto a Phenomenex Luna 250 × 30 mm, 5 μm, C_{18} column at room temperature. The flow rate was 40 mL/min. A linear gradient was used with 10% acetonitrile in H_2O (with 0.1% TFA) (B) to 100% of acetonitrile (A). HPLC was used to establish the purity of target compounds. All final compounds had >96% purity using the HPLC methods described above. MS4048[38] and intermediate **2−4**[35] were synthesized according to the published procedures.

Synthesis of 2-((2-azidoethyl)disulfanyl)ethyl 3-(4-amino-1,3-dioxoisoindolin-2-yl)-2,6-dioxopiperidine-1-carboxylate (5). To a solution of pomalidomide (55.0 mg, 0.2 mmol, 1.0 equiv) in dimethylformamide (DMF) (2 mL) was added NaH (9.6 mg, 60% in mineral oil, 0.24 mmol, 1.2 equiv) at 0 °C. After stirring for 10 min, 2-((2-azidoethyl)disulfanyl)ethyl carbonochloridate (see reference[50] for the details of synthesis) (58.0 mg, 0.24 mmol, 1.2 equiv) was added to the mixture at 0 °C. The reaction mixture was then warmed to room temperature and stirred for additional 2 h. The resulting mixture was purified by preparative HPLC (10−100% acetonitrile/0.1% trifluoroacetic acid, TFA, in H_2O). The product-containing fractions were concentrated to remove the organic solvent under reduced pressure

and then dried by lyophilization to afford compound **5** as a yellow solid (45.9 mg, 48%). ^{1}H NMR (600 MHz, DMSO-d_6) δ 7.49 (t, J = 7.7 Hz, 1H), 7.06−7.00 (m, 2H), 6.56 (s, 2H), 5.37 (dd, J = 12.9, 5.4 Hz, 1H), 4.65−4.48 (m, 2H), 3.60 (t, J = 6.4 Hz, 2H), 3.18−3.02 (m, 3H), 2.95 (t, J = 6.5 Hz, 2H), 2.83 (d, J = 18.1 Hz, 1H), 2.68−2.55 (m, 1H), 2.19−2.04 (m, 1H). ESI m/z = 501.1 [M + Na]$^+$.

Synthesis of N^5-((1-(2-((2-((3-(4-amino-1,3-dioxoisoindolin-2-yl)-2,6-dioxopiperidin-1-carbonyl)oxy)ethyl)disulfanyl)-ethyl)-1H-1,2,3-triazol-4-yl)methyl)-N^2-(4-(((2-amino-4-oxo-3,4-dihydropteridin-6-yl)methyl)amino)benzoyl)-L-glutamine (FA-S2-POMA). To a solution of compound **5** (24.0 mg, 0.05 mmol, 1.0 equiv) in DMF (1.6 mL)/water (0.8 mL) were added compound **4** (28.8 mg, 0.06 mmol, 1.2 equiv), sodium ascorbate (2.9 mg, 0.015 mmol, 0.3 equiv), and CuSO$_4$.5H$_2$O (1.3 mg, 0.007 mmol, 0.15 equiv) at room temperature. The reaction mixture was heated to 50 °C. After being stirred at 50 °C for 2 h, the resulting mixture was purified by preparative HPLC (10−100% acetonitrile/0.1% TFA in H$_2$O). The product-containing fractions were concentrated to remove the organic solvent under reduced pressure at room temperature and then dried by lyophilization to afford **FA-S2-POMA** as a yellow solid (15.9 mg, 33%). ^{1}H NMR (600 MHz, DMSO-d_6) δ 8.61 (s, 1H), 8.29 (t, J = 5.8 Hz, 1H), 8.13 (d, J = 7.6 Hz, 1H), 7.84 (s, 1H), 7.59 (d, J = 8.4 Hz, 2H), 7.48−7.35 (m, 1H), 7.07−6.89 (m, 2H), 6.58 (d, J = 8.4 Hz, 2H), 6.54−6.42 (m, 2H), 5.30 (dd, J = 12.9, 5.4 Hz, 1H), 4.58−4.38 (m, 6H), 4.32−4.10 (m, 3H), 3.14 (t, J = 6.6 Hz, 2H), 3.05 (ddd, J = 18.4, 13.7, 5.5 Hz, 1H), 2.99 (t, J = 6.3 Hz, 2H), 2.76 (dt, J = 17.7, 3.5 Hz, 1H), 2.54 (qd, J = 13.3, 4.5 Hz, 1H), 2.24−2.12 (m, 2H), 2.09−1.98 (m, 2H), 1.89−1.80 (m, 1H). ^{13}C NMR (151 MHz, DMSO-d_6) δ 174.29, 172.03, 170.61, 168.73, 168.32, 167.62, 166.87, 161.45, 156.06, 154.25, 151.22, 150.94, 149.35, 149.04, 147.30, 145.63, 136.10, 132.32, 129.46, 123.40, 122.36, 121.77, 111.67, 111.63, 108.77, 67.22, 52.54, 48.75, 48.38, 46.36, 37.43, 35.87, 34.66, 32.25, 31.19, 26.92, 21.73. HRMS (ESI-TOF) calcd for C$_{40}$H$_{41}$N$_{14}$O$_{11}$S$_2$$^+$ [M + H]$^+$ 957.2515, found 957.2507. HPLC >98%, tR = 3.80 min.

Synthesis of 6-azidohexyl 3-(4-amino-1,3-dioxoisoindolin-2-yl)-2,6-dioxopiperidine-1-carboxylate (6). To a solution of pomalidomide (109.3 mg, 0.4 mmol, 1.0 equiv) in DMF (2 mL) was added NaH (19.2 mg, 60% in mineral oil, 0.48 mmol, 1.2 equiv) at 0 °C. After stirring for 10 min, 6-azidohexyl carbonochloridate (see reference[50] for the details of synthesis) (99.0 mg, 0.48 mmol, 1.2 equiv) was added to the mixture at 0 °C. The reaction mixture was then warmed to room temperature and stirred for additional 2 h. The resulting mixture was purified by preparative HPLC (10−100% acetonitrile/0.1% TFA in H$_2$O). The product-containing fractions were concentrated to remove the organic solvent under reduced pressure and then dried by lyophilization to afford compound **6** as a yellow solid (60.2 mg, 34%). ^{1}H NMR (600 MHz, DMSO-d_6) δ 7.53−7.45 (m, 1H), 7.06−6.99 (m, 2H), 6.56 (s, 2H), 5.36 (dd, J = 12.9, 5.3 Hz, 1H), 4.47−4.26 (m, 2H), 3.30 (t, J = 6.9 Hz, 2H), 3.16−3.06 (m, 1H), 2.86−2.76 (m, 1H), 2.60 (qd, J = 13.3, 4.4 Hz, 1H), 2.14−2.07 (m, 1H), 1.72−1.63 (m, 2H), 1.56−1.48 (m, 2H), 1.42−1.29 (m, 4H). ESI m/z = 465.2 [M + Na]$^+$.

Synthesis of N^5-((1-(6-((3-(4-amino-1,3-dioxoisoindolin-2-yl)-2,6-dioxopiperidin-1-carbonyl)oxy)hexyl)-1H-1,2,3-triazol-4-yl)methyl)-N^2-(4-(((2-amino-4-oxo-3,4-dihydropteridin-6-yl)methyl)amino)benzoyl)-L-glutamine (FA-C2-POMA). To a solution of compound **6** (15.9 mg, 0.036 mmol, 1.2 equiv) in DMF (1.6 mL)/water (0.8 mL) were added compound **4** (14.4 mg, 0.03 mmol, 1.0 equiv), sodium ascorbate (2.4 mg, 0.012 mmol, 0.4 equiv), and CuSO$_4$.5H$_2$O (1.5 mg, 0.006 mmol, 0.2 equiv) at room temperature. The reaction mixture was heated to 50 °C. After being stirred at 50 °C for 2 h, the resulting mixture was purified by preparative HPLC (10−100% acetonitrile/0.1% TFA in H$_2$O). The product-containing fractions were concentrated to remove the organic solvent under reduced pressure at room temperature and then dried by lyophilization to afford **FA-C2-POMA** as a yellow solid (13.6 mg, 49%). ^{1}H NMR (600 MHz, DMSO-d_6) δ 8.62 (s, 1H), 8.26 (t, J = 5.7 Hz, 1H), 8.13 (d, J = 7.7 Hz, 1H), 7.78 (s, 1H), 7.59 (d, J = 8.6 Hz, 2H), 7.40 (t, J = 7.8 Hz, 1H), 6.99−6.90 (m, 2H), 6.58 (d, J = 8.0 Hz, 2H), 5.28 (dd, J = 13.1, 5.0 Hz, 1H), 4.45 (s, 2H), 4.35−4.13 (m,

7H), 3.11−2.97 (m, 1H), 2.79−2.71 (m, 1H), 2.59−2.48 (m, 1H), 2.28−2.13 (m, 2H), 2.10−1.97 (m, 2H), 1.94−1.81 (m, 1H), 1.76−1.64 (m, 2H), 1.61−1.49 (m, 2H), 1.37−1.25 (m, 2H), 1.23−1.10 (m, 2H). ^{13}C NMR (151 MHz, DMSO-d_6) δ 174.31, 171.98, 170.64, 168.73, 168.35, 167.61, 166.82, 161.00, 154.47, 153.97, 151.18, 150.94, 150.02, 148.83, 147.31, 145.41, 136.07, 132.34, 129.45, 123.05, 122.34, 121.85, 111.68, 111.59, 108.78, 69.61, 52.55, 49.58, 48.74, 46.33, 34.73, 32.26, 31.19, 30.00, 27.94, 26.92, 25.76, 24.76, 21.79. HRMS (ESI-TOF) calcd for C$_{42}$H$_{45}$N$_{14}$O$_{11}$$^+$ [M + H]$^+$ 921.3387, found 921.3386. HPLC >96%, tR = 3.79 min.

Synthesis of N^2-(4-(((2-amino-4-oxo-3,4-dihydropteridin-6-yl)methyl)amino)benzoyl)-N^5-((1-(2-mercaptoethyl)-1H-1,2,3-triazol-4-yl)methyl)-L-glutamine (Folate-SH). To a solution of **FA-S2-POMA** (9.6 mg, 0.01 mmol, 1.0 equiv) in DMSO (1.0 mL) was added DTT (4.6 mg, 0.03 mmol, 3.0 equiv) at room temperature. The reaction mixture was heated to 37 °C. After being stirred at 37 °C for 20 min, the resulting mixture was purified by preparative HPLC (10−100% acetonitrile/0.1% TFA in H$_2$O). The product-containing fractions were concentrated to remove the organic solvent under reduced pressure at room temperature and then dried by lyophilization to afford **Folate-SH** as a yellow solid (4.3 mg, 74%). ^{1}H NMR (600 MHz, DMSO-d_6) δ 12.40 (s, 1H), 8.58 (s, 1H), 8.27 (t, J = 5.7 Hz, 1H), 8.12 (d, J = 7.7 Hz, 1H), 7.83 (s, 1H), 7.58 (d, J = 8.4 Hz, 2H), 6.57 (d, J = 8.5 Hz, 2H), 4.42 (s, 2H), 4.38 (t, J = 6.9 Hz, 2H), 4.29−4.14 (m, 3H), 2.86 (q, J = 7.3 Hz, 2H), 2.38 (t, J = 8.3 Hz, 1H), 2.21−2.12 (m, 2H), 2.04−1.98 (m, 1H), 1.90−1.78 (m, 1H). ESI m/z = 582.2 [M + H]$^+$.

Synthesis of 2-((2-azidoethyl)disulfanyl)ethyl 3-(4-((2-aminoethyl)amino)-1,3-dioxoisoindolin-2-yl)-2,6-dioxopiperidine-1-carboxylate (8). To a solution of tert-butyl (2-((2-(2,6-dioxopiperidin-3-yl)-1,3-dioxoisoindolin-4-yl)amino)ethyl)carbamate (**7**) (see reference[38] for the details of synthesis) (62.5 mg, 0.15 mmol, 1.0 equiv) in DMF (2 mL) was added NaH (9.0 mg, 60% in mineral oil, 0.225 mmol, 1.5 equiv) at 0 °C. After stirring for 10 min, 2-((2-azidoethyl)disulfanyl)ethyl carbonochloridate (55.0 mg, 0.225 mmol, 1.5 equiv) was added to the mixture at 0 °C. The reaction mixture was then warmed to room temperature and stirred for additional 1 h. The resulting mixture was purified by preparative HPLC (10−100% acetonitrile/0.1% TFA in H$_2$O). The product-containing fractions were concentrated to remove the organic solvent under reduced pressure and then dried by lyophilization to afford the desired intermediate as a yellow solid. ESI m/z = 644.2 [M + Na]$^+$. To a solution of above-obtained compound in CH$_2$Cl$_2$ (2 mL) was added TFA (1 mL) at room temperature. After stirring for 1 h, the resulting mixture was concentrated and purified by preparative HPLC (10−100% acetonitrile/0.1% TFA in H$_2$O). The product-containing fractions were concentrated to remove the organic solvent under reduced pressure and then dried by lyophilization to afford **8** as a yellow solid in the TFA salt form (26.0 mg, 27%). ^{1}H NMR (600 MHz, Methanol-d_4) δ 7.55−7.47 (m, 1H), 7.08−7.01 (m, 2H), 5.18−5.14 (m, 1H), 4.54−4.42 (m, 2H), 3.65−3.56 (m, 2H), 3.53−3.45 (m, 2H), 3.16−3.07 (m, 2H), 3.02−2.66 (m, 7H), 2.14−2.02 (m, 1H). ESI m/z = 522.3 [M + H]$^+$.

Synthesis of 2-((2-azidoethyl)disulfanyl)ethyl 3-(4-((2-(2-(4-(4-((5-chloro-4-((2-(isopropylsulfonyl)phenyl)amino)-pyrimidin-2-yl)amino)-5-isopropoxy-2-methylphenyl)-piperidin-1-yl)acetamido)ethyl)amino)-1,3-dioxoisoindolin-2-yl)-2,6-dioxopiperidine-1-carboxylate (10). To a solution of compound **8** (26.0 mg, 0.041 mmol, 1.0 equiv) in dimethyl sulfoxide (DMSO) (4 mL) were added compound **9** (2-(4-(4-((5-chloro-4-((2-(isopropylsulfonyl)phenyl)amino)pyrimidin-2-yl)amino)-5-iso-propoxy-2-methylphenyl)piperidin-1-yl)acetic acid) (see reference 3 for the details of synthesis) (27.8 mg, 0.045 mmol, 1.1 equiv), EDCI (1-ethyl-3-(3-dimethylaminopropyl)carbodiimide) (16.0 mg, 0.082 mmol, 2.0 equiv), HOAt (1-hydroxy-7-azabenzo-triazole) (11.2 mg, 0.082 mmol, 2.0 equiv), and NMM (N-methylmorpholine) (20.7 mg, 0.205 mmol, 5.0 equiv). After being stirred at room temperature for 4 h, the resulting mixture was purified by preparative HPLC (10−100% acetonitrile/0.1% TFA in H$_2$O). The product-containing fractions were concentrated to remove the organic solvent under reduced pressure at room temperature and then dried by lyophilization to

afford compound **10** as a brown solid in the TFA salt form (28.0 mg, 55%). ^{1}H NMR (600 MHz, methanol-d_4) δ 8.26 (d, J = 8.3 Hz, 1H), 8.14 (s, 1H), 7.89 (d, J = 8.5 Hz, 1H), 7.63 (t, J = 7.9 Hz, 1H), 7.53–7.47 (m, 2H), 7.39 (t, J = 7.7 Hz, 1H), 7.08 (d, J = 8.6 Hz, 1H), 7.01 (d, J = 7.1 Hz, 1H), 6.79 (s, 1H), 5.12 (dd, J = 12.8, 5.4 Hz, 1H), 4.54 (p, J = 6.1 Hz, 1H), 4.40–4.29 (m, 2H), 3.84 (s, 2H), 3.63–3.42 (m, 8H), 3.34–3.25 (m, 1H), 3.11 (t, J = 12.4 Hz, 2H), 3.04–2.96 (m, 1H), 2.93–2.82 (m, 3H), 2.82–2.72 (m, 3H), 2.65 (qd, J = 13.3, 4.4 Hz, 1H), 2.17–1.84 (m, 8H), 1.24 (d, J = 6.0 Hz, 6H), 1.17 (d, J = 6.8 Hz, 6H). ESI m/z = 1119.3 [M + H]+.

Synthesis of N^2-(4-(((2-amino-4-oxo-3,4-dihydropteridin-6-yl)methyl)amino)benzoyl)-N^5-((1-(2-((2-((2-((3-(4-((2-(2-(4-(4-((5-chloro-4-((2-(isopropylsulfonyl)phenyl)amino)pyrimidin-2-yl)amino)-5-isopropoxy-2-methylphenyl)piperidin-1-yl)-acetamido)ethyl)amino)-1,3-dioxoisoindolin-2-yl)-2,6-dioxo-piperidine-1-carbonyl)oxy)ethyl)disulfanyl)ethyl)-1H-1,2,3-tri-azol-4-yl)methyl)-L-glutamine (FA-S2-MS4048). To a solution of compound **10** (28.0 mg, 0.023 mmol, 1.0 equiv) in DMF (1.6 mL)/water (0.8 mL) were added compound **4** (13.0 mg, 0.027 mmol, 1.2 equiv), sodium ascorbate (1.8 mg, 0.009 mmol, 0.4 equiv), and CuSO$_4$.5H$_2$O (1.2 mg, 0.005 mmol, 0.2 equiv) at room temperature. The reaction mixture was heated to 50 °C. After being stirred at 50 °C for 2 h, the resulting mixture was purified by preparative HPLC (10–100% acetonitrile/0.1% TFA in H$_2$O). The product-containing fractions were concentrated to remove the organic solvent under reduced pressure at room temperature and then dried by lyophilization to afford **FA-S2-MS4048** as a yellow solid in the TFA salt form (12.7 mg, 32%). ^{1}H NMR (600 MHz, DMSO-d_6) δ 9.67 (s, 1H), 9.55 (s, 1H), 8.85 (t, J = 5.8 Hz, 1H), 8.70 (s, 1H), 8.43 (d, J = 8.2 Hz, 1H), 8.37 (t, J = 5.8 Hz, 1H), 8.28 (s, 1H), 8.24 (s, 1H), 8.21 (d, J = 7.7 Hz, 1H), 7.92 (s, 1H), 7.86 (d, J = 8.0 Hz, 1H), 7.69–7.58 (m, 4H), 7.52 (s, 1H), 7.38 (t, J = 7.6 Hz, 1H), 7.22 (d, J = 8.7 Hz, 2H), 7.07 (d, J = 7.1 Hz, 1H), 6.80 (s, 2H), 6.65 (d, J = 8.5 Hz, 2H), 5.39 (dd, J = 12.9, 5.6 Hz, 1H), 4.63–4.46 (m, 7H), 4.36–4.20 (m, 3H), 3.94 (s, 2H), 3.58–3.34 (m, 8H), 3.28–3.16 (m, 3H), 3.16–3.07 (m, 1H), 3.04 (t, J = 6.3 Hz, 2H), 2.99–2.90 (m, 1H), 2.85–2.77 (m, 1H), 2.66–2.55 (m, 1H), 2.30–2.18 (m, 2H), 2.18–2.00 (m, 7H), 1.94–1.83 (m, 3H), 1.26 (d, J = 6.0 Hz, 6H), 1.16 (d, J = 6.8 Hz, 6H). ^{13}C NMR (151 MHz, DMSO-d_6) δ 174.30, 171.99, 170.55, 168.91, 168.28, 167.48, 166.82, 165.08, 160.65, 157.92, 155.63, 154.95, 153.76, 151.16, 150.92, 150.53, 148.68, 147.28, 146.79, 145.66, 138.34, 138.11, 136.91, 135.27, 132.60, 131.48, 129.47, 128.45, 127.45, 127.19, 125.42, 124.54, 124.47, 124.36, 123.38, 121.87, 117.71, 111.83, 111.69, 111.38, 109.67, 104.91, 71.34, 67.19, 57.38, 55.27, 53.56, 52.54, 48.80, 48.38, 46.30, 41.73, 40.51, 38.64, 37.42, 35.87, 34.67, 32.25, 31.18, 29.52, 26.93, 22.34, 21.76, 18.79, 15.30. HRMS (ESI-TOF) calcd for C$_{72}$H$_{82}$ClN$_{20}$O$_{15}$S$_3^+$ [M + H]+ 1597.5114, found 1597.5101. HPLC >96%, tR = 4.42 min.

Synthesis of 6-azidohexyl 3-(4-((2-aminoethyl)amino)-1,3-dioxoisoindolin-2-yl)-2,6-dioxopiperidine-1-carboxylate (11). To a solution of *tert*-butyl (2-((2-(2,6-dioxopiperidin-3-yl)-1,3-dioxoisoindolin-4-yl)amino)ethyl)carbamate (**7**) (62.5 mg, 0.15 mmol, 1.0 equiv) in DMF (2 mL) was added NaH (9.0 mg, 60% in mineral oil, 0.225 mmol, 1.5 equiv) at 0 °C. After stirring for 10 min, 2-((2-azidoethyl)disulfanyl)ethyl carbonochloridate (46.3 mg, 0.225 mmol, 1.5 equiv) was added to the mixture at 0 °C. The reaction mixture was then warmed to room temperature and stirred for additional 1 h. The resulting mixture was purified by preparative HPLC (10–100% acetonitrile/0.1% TFA in H$_2$O). The product-containing fractions were concentrated to remove the organic solvent under reduced pressure and then dried by lyophilization to afford the desired intermediate as a yellow solid. ESI m/z = 608.3 [M + Na]+. To a solution of the obtained abovementioned compound in CH$_2$Cl$_2$ (2 mL) was added TFA (1 mL) at room temperature. After stirring for 1 h, the resulting mixture was concentrated and purified by preparative HPLC (10–100% acetonitrile/0.1% TFA in H$_2$O). The product-containing fractions were concentrated to remove the organic solvent under reduced pressure and then dried by lyophilization to afford **11** as a yellow solid in the TFA salt form (40.0 mg, 44%). ^{1}H NMR (600 MHz, methanol-d_4) δ 7.62 (dd, J = 8.5, 7.2 Hz, 1H), 7.15

(d, J = 7.8 Hz, 2H), 5.24 (dd, J = 12.9, 5.4 Hz, 1H), 4.38–4.30 (m, 2H), 3.69 (t, J = 6.1 Hz, 2H), 3.26 (t, J = 6.9 Hz, 2H), 3.20 (t, J = 6.1 Hz, 2H), 3.01 (ddd, J = 17.6, 13.7, 5.3 Hz, 1H), 2.91 (ddd, J = 17.6, 4.5, 2.7 Hz, 1H), 2.79 (qd, J = 13.2, 4.5 Hz, 1H), 2.19–2.11 (m, 1H), 1.76–1.66 (m, 2H), 1.57 (p, J = 7.0 Hz, 2H), 1.47–1.33 (m, 4H). ESI m/z = 486.3 [M + H]+.

Synthesis of 6-azidohexyl 3-(4-((2-(2-(4-(4-((5-chloro-4-((2-(isopropylsulfonyl)phenyl)amino)pyrimidin-2-yl)amino)-5-iso-propoxy-2-methylphenyl)piperidin-1-yl)acetamido)ethyl)-amino)-1,3-dioxoisoindolin-2-yl)-2,6-dioxopiperidine-1-car-boxylate (12). To a solution of compound **11** (40.0 mg, 0.067 mmol, 1.0 equiv) in DMSO (4 mL) were added compound **9** (53.3 mg, 0.073 mmol, 1.1 equiv), EDCI (25.7 mg, 0.134 mmol, 2.0 equiv), HOAt (18.2 mg, 0.134 mmol, 2.0 equiv), and NMM (34.0 mg, 0.335 mmol, 5.0 equiv). After being stirred at room temperature for 4 h, the resulting mixture was purified by preparative HPLC (10–100% acetonitrile/0.1% TFA in H$_2$O). The product-containing fractions were concentrated to remove the organic solvent under reduced pressure and then dried by lyophilization to afford compound **12** as a brown solid in the TFA salt form (60.1 mg, 75%). ^{1}H NMR (600 MHz, methanol-d_4) δ 8.21 (d, J = 8.3 Hz, 1H), 8.12 (s, 1H), 7.87 (dd, J = 7.9, 1.6 Hz, 1H), 7.64–7.56 (m, 1H), 7.47 (dd, J = 8.6, 7.1 Hz, 1H), 7.43–7.34 (m, 2H), 7.05 (d, J = 8.6 Hz, 1H), 6.97 (d, J = 7.1 Hz, 1H), 6.78 (s, 1H), 5.09 (dd, J = 12.8, 5.4 Hz, 1H), 4.53 (p, J = 6.1 Hz, 1H), 4.18–4.04 (m, 2H), 3.83 (s, 2H), 3.56 (t, J = 11.0 Hz, 2H), 3.47 (t, J = 5.9 Hz, 2H), 3.44–3.40 (m, 2H), 3.33–3.22 (m, 1H), 3.16–3.08 (m, 4H), 3.02–2.96 (m, 1H), 2.86 (ddd, J = 17.5, 13.7, 5.3 Hz, 1H), 2.74 (ddd, J = 17.6, 4.5, 2.8 Hz, 1H), 2.62 (qd, J = 13.2, 4.4 Hz, 1H), 2.07 (s, 3H), 2.02–1.84 (m, 5H), 1.57–1.49 (m, 2H), 1.42 (p, J = 7.0 Hz, 2H), 1.29–1.22 (m, 4H), 1.21 (d, J = 6.0 Hz, 6H), 1.14 (d, J = 6.8 Hz, 6H). ESI m/z = 1083.5 [M + H]+.

Synthesis of N^2-(4-(((2-amino-4-oxo-3,4-dihydropteridin-6-yl)methyl)amino)benzoyl)-N^5-((1-(6-((3-(4-((2-(2-(4-(4-((5-chloro-4-((2-(isopropylsulfonyl)phenyl)amino)pyrimidin-2-yl)-amino)-5-isopropoxy-2-methylphenyl)piperidin-1-yl)-acetamido)ethyl)amino)-1,3-dioxoisoindolin-2-yl)-2,6-dioxo-piperidine-1-carbonyl)oxy)hexyl)-1H-1,2,3-triazol-4-yl)-methyl)-L-glutamine (FA-C2-MS4048). To a solution of compound **12** (26.0 mg, 0.022 mmol, 1.0 equiv) in DMF (1.6 mL)/water (0.8 mL) were added compound **4** (12.5 mg, 0.026 mmol, 1.2 equiv), sodium ascorbate (1.7 mg, 0.009 mmol, 0.4 equiv), and CuSO$_4$.5H$_2$O (1.1 mg, 0.004 mmol, 0.2 equiv) at room temperature. The reaction mixture was heated to 50 °C. After being stirred at 50 °C for 2 h, the resulting mixture was purified by preparative HPLC (10–100% acetonitrile/0.1% TFA in H$_2$O). The product-containing fractions were concentrated to remove the organic solvent under reduced pressure at room temperature and then dried by lyophilization to afford **FA-C2-MS4048** as a yellow solid in the TFA salt form (14.9 mg, 40%). ^{1}H NMR (600 MHz, DMSO-d_6) δ 9.60 (s, 1H), 9.50 (s, 1H), 8.77 (t, J = 5.7 Hz, 1H), 8.64 (s, 1H), 8.35 (d, J = 8.3 Hz, 1H), 8.26 (t, J = 5.8 Hz, 1H), 8.24–8.19 (m, 2H), 8.14 (d, J = 7.6 Hz, 1H), 7.85–7.74 (m, 2H), 7.64–7.51 (m, 4H), 7.44 (s, 1H), 7.31 (t, J = 7.6 Hz, 1H), 7.14 (d, J = 8.6 Hz, 1H), 6.99 (d, J = 7.1 Hz, 1H), 6.73 (s, 2H), 6.58 (d, J = 8.3 Hz, 2H), 5.29 (dd, J = 12.8, 5.6 Hz, 1H), 4.54–4.39 (m, 3H), 4.30–4.11 (m, 7H), 3.86 (s, 2H), 3.53–3.26 (m, 7H), 3.20–3.08 (m, 2H), 3.07–2.98 (m, 1H), 2.88 (t, J = 12.3 Hz, 1H), 2.75–2.66 (m, 1H), 2.57–2.46 (m, 1H), 2.27–2.09 (m, 2H), 2.11–1.94 (m, 7H), 1.91–1.81 (m, 1H), 1.81–1.74 (m, 2H), 1.72–1.65 (m, 2H), 1.62–1.47 (m, 2H), 1.34–1.12 (m, 10H), 1.09 (d, J = 6.8 Hz, 6H). ^{13}C NMR (151 MHz, DMSO-d_6) δ 174.31, 171.97, 170.58, 168.91, 168.31, 167.47, 166.79, 165.08, 160.40, 157.71, 155.74, 154.54, 153.58, 151.13, 150.90, 148.56, 147.28, 146.78, 145.40, 138.27, 138.19, 136.88, 135.27, 132.60, 131.49, 129.45, 128.42, 127.33, 127.18, 125.58, 124.60, 124.54, 124.47, 123.02, 121.91, 117.70, 111.81, 111.70, 111.35, 109.67, 104.92, 71.34, 69.60, 57.37, 55.26, 53.55, 52.55, 49.56, 48.78, 46.27, 41.75, 40.50, 38.63, 34.73, 34.66, 32.25, 31.16, 30.00, 29.51, 27.93, 26.93, 25.76, 24.75, 22.33, 21.81, 18.78, 15.29. HRMS (ESI-TOF) calcd for C$_{74}$H$_{86}$ClN$_{20}$O$_{15}$S$^+$ [M + H]+ 1561.5985, found 1561.5960. HPLC >97%, tR = 4.45 min.

***In Vitro* Drug Release.** Folate conjugates (FA-S2-POMA, FA-C2-POMA, FA-S2-MS4048, or FA-C2-MS4048) in DMSO (2 mM, 10 μL) were diluted to 200 μM with PBS (90 μL). After the addition of DTT (400 μM, 100 μL for FA-S2-POMA and FA-C2-POMA, 2 mM, 100 μL for FA-S2-MS4048 and FA-C2-MS4048), the mixture was incubated at 37 °C. At the indicated time, samples were withdrawn and analyzed by HPLC.

Cell Culture. Human embryonic kidney 293T (HEK293T) and MM.1S cells were maintained in Dulbecco's modified Eagle's medium (DMEM) containing 10% fetal bovine serum (FBS), 100 units/mL of penicillin, and 100 μg/mL streptomycin. SU-DHL-1, THP-1, NCI-H2228, and NCI-H3122 cells were cultured in RPMI1640 containing 10% FBS, 100 units/mL of penicillin, and 100 μg/mL streptomycin. The usage of MM.1S cells for evaluation of pomalidomide, as well as the usage of SU-DHL-1, NCI-H2228, and NCI-H3122 cells for the evaluation of the ALK degrader are based on our previous reports.[35,37] MM.1S-CRBN$^{+/+}$ and MM.1S-CRBN$^{-/-}$ cells were kindly gifted by Dr. William Kaelin, Jr. at Dana-Farber Cancer Institute, Harvard Medical School. SU-DHL-1-CRBN$^{-/-}$ cells were generated using CRISPR-Cas9 technology with sgRNA as given below: sg #1: TAAACAGACATGGCCGGCGA, sg #2: GTCCTGCTGATCTCCTTCGC, and sg #3: CAGGACGCTGCG-CACAACAT. The shRNA for FOLR1 was purchased from Sigma-Aldrich. The lentiviruses of sgCRBN and shFOLR1 were generated in HEK293T cells for the infection of SU-DHL-1 cells, as previously described.[51] Cells were infected with lentivirus and selected with puromycin for 72 h, followed by the drug treatment.

For folic acid competitive degradation assay, cells were pretreated with folic acid (F8758, Sigma-Aldrich, 2.5 mM) for 2 h, followed by the treatment of indicated PROTACs for the indicated time. For endocytosis inhibition, cells were pretreated with MβCD (21,633, Cayman, 30 μM–1 mM) for 12 h, followed by cotreatment with indicated compounds for another 12 h. For proteasome or E3 ligase inhibition assay, cells were treated with MG132 (BML-Pl1020, ENZO Life Sciences, 10 μM) or MLN4924 (S7109, SelleckChem, 1 μM) for 12 h. For GSH-stimulating assay, cells were treated with S-acetyl-GSH (29,624, Cayman, 1 mM) with indicated compounds for 12 or 72 h.

Immunoblot Assay. Cells were lysed in EBC buffer (50 mM Tris−HCl pH 7.5, 120 mM NaCl, 0.5% NP-40) supplemented with protease inhibitors (Pierce) and phosphatase inhibitors (phosphatase inhibitor cocktail set I and II, Calbiochem). The protein concentrations of the lysates were measured using the Bio-Rad protein assay reagent on a Beckman Coulter DU-800 spectrophotometer. The lysates (40 μg of protein) were then resolved by 10% sodium dodecyl sulfate−polyacrylamide gel (SDS−PAGE) electrophoresis at 130 V for 80 min and immunoblotted with indicated antibodies at 4 °C overnight, washed four times with tris-buffered saline with 0.1% Tween-20 (TBST), incubated with secondary antibody for 1 h at room temperature, and then washed 4 times with TBST. All western blot assays were repeated at least twice, and a representative result is shown in figures.

Antibodies. Anti-IKZF1 (ab191394, 1:1000) antibody was purchased from Abcam. Anti-IKZF3 (NBP22449, 1:1000) antibody was purchased from Novus Biologicals. Anti-ALK (3633, 1:1000) and anti-CRBN (71,810, 1:1000) were purchased from Cell Signaling Technologies. Anti-FOLR1 (23355-1-AP, 1:1000) antibodies was purchased from Proteintech. Monoclonal anti-Flag antibody (F-3165, 1:5000), anti-Vinculin antibody (V-4505; 1:50,000), peroxidase-conjugated anti-mouse secondary antibody (A-4416; 1:5000), and peroxidase-conjugated anti-rabbit secondary antibody (A-4914; 1:5000) were purchased from Sigma-Aldrich. All primary antibodies were prepared in 5% bovine serum albumin (BSA) in the TBST buffer and secondary antibodies were prepared in 5% nonfat milk in the TBST buffer.

Streptavidin Pulldown Assay. The streptavidin pulldown assay for biotin-pomalidomide was performed, as previously reported.[37] Briefly, flag-CRBN was expressed in the HEK293T cells lysed in PROTAC buffer B (50 mM Tris−HCl, pH 7.5, 150 mM NaCl, and 0.5% NP-40) supplemented with protease inhibitors and phosphatase inhibitors. A total of 1 mg of cell lysate was incubated with 10 μL of 10 mM biotin-pomalidomide and 8 μL of streptavidin beads for 1 h at 4 °C in the absence or presence of pomalidomide or its derivates. Alternatively, folate-S2-pomalidomide or folate-C2-pomalidomide was incubated with 5 mM GSH and then subjected to the competition binding assay. Then, the beads were washed four times with the wash buffer (20 mM Tris−HCl, pH 7.5, pH 8.0, 100 mM NaCl, 1 mM EDTA, and 0.5% NP-40), before being resolved using SDS-PAGE and immunoblotted with the flag-tag antibody.

CCK-8 Cell Proliferation Assay. Cell viability was analyzed, as previously described.[35,37] Briefly, cells were treated with the indicated concentrations of test compounds for 72 h and then incubated with 10 μL/well of CCK-8 (K1018, APExBIO) solution at 37 °C for 2 h, followed by the measurement of optical density at 450 nm (OD450).

■ ASSOCIATED CONTENT

ⓢ Supporting Information

The Supporting Information is available free of charge at https://pubs.acs.org/doi/10.1021/acs.jmedchem.1c00901.

> Synthetic scheme of folate-SH, degradation effects of FA-S2-POMA and FA-S2-MS4048 in cells, and ^{1}H NMR, ^{13}C NMR, and LC−MS spectra of FA-S2-POMA, FA-C2-POMA, FA-S2-MS4048, and FA-C2-MS4048 (PDF)

> Molecular formula strings for all compounds (CSV)

■ AUTHOR INFORMATION

Corresponding Authors

Wenyi Wei − *Department of Pathology, Beth Israel Deaconess Medical Center, Harvard Medical School, Boston, Massachusetts 02215, United States;* ⓞ orcid.org/0000-0003-0512-3811; Email: wwei2@bidmc.harvard.edu

Jian Jin − *Mount Sinai Center for Therapeutics Discovery, Departments of Pharmacological Sciences and Oncological Sciences, Tisch Cancer Institute, Icahn School of Medicine at Mount Sinai, New York, New York 10029, United States;* ⓞ orcid.org/0000-0002-2387-3862; Email: jian.jin@mssm.edu

Authors

He Chen − *Mount Sinai Center for Therapeutics Discovery, Departments of Pharmacological Sciences and Oncological Sciences, Tisch Cancer Institute, Icahn School of Medicine at Mount Sinai, New York, New York 10029, United States*

Jing Liu − *Department of Pathology, Beth Israel Deaconess Medical Center, Harvard Medical School, Boston, Massachusetts 02215, United States*

H. Ümit Kaniskan − *Mount Sinai Center for Therapeutics Discovery, Departments of Pharmacological Sciences and Oncological Sciences, Tisch Cancer Institute, Icahn School of Medicine at Mount Sinai, New York, New York 10029, United States;* ⓞ orcid.org/0000-0001-5327-832X

Complete contact information is available at:
https://pubs.acs.org/10.1021/acs.jmedchem.1c00901

■ ABBREVIATIONS

FOLR1, folate receptor α; GSH, glutathione; DTT, dithiothreitol; S-Ac-GSH, S-acetyl-L-glutathione; ALK, anaplastic lymphoma kinase; DMF, dimethylformamide; NaH, sodium hydride; TFA, trifluoroacetic acid; EDCI, 1-ethyl-3-(3-dimethylaminopropyl)carbodiimide; HOAt, 1-hydroxy-7-aza-benzo-triazole; NMM, N-methylmorpholine; DMSO, dimethyl sulfoxide; ESI, electrospray ionization.

■ REFERENCES

(1) Chamberlain, P. P.; Hamann, L. G. Development of targeted protein degradation therapeutics. Nat. Chem. Biol. 2019, 15, 937−944.

(2) Ito, T.; Ando, H.; Suzuki, T.; Ogura, T.; Hotta, K.; Imamura, Y.; Yamaguchi, Y.; Handa, H. Identification of a primary target of thalidomide teratogenicity. Science 2010, 327, 1345−1350.

(3) Kronke, J.; Udeshi, N. D.; Narla, A.; Grauman, P.; Hurst, S. N.; McConkey, M.; Svinkina, T.; Heckl, D.; Comer, E.; Li, X.; Ciarlo, C.; Hartman, E.; Munshi, N.; Schenone, M.; Schreiber, S. L.; Carr, S. A.; Ebert, B. L. Lenalidomide causes selective degradation of IKZF1 and IKZF3 in multiple myeloma cells. Science 2014, 343, 301−305.

(4) Lu, G.; Middleton, R. E.; Sun, H.; Naniong, M.; Ott, C. J.; Mitsiades, C. S.; Wong, K. K.; Bradner, J. E.; Kaelin, W. G., Jr. The myeloma drug lenalidomide promotes the cereblon-dependent destruction of Ikaros proteins. Science 2014, 343, 305−309.

(5) Han, T.; Goralski, M.; Gaskill, N.; Capota, E.; Kim, J.; Ting, T. C.; Xie, Y.; Williams, N. S.; Nijhawan, D. Anticancer sulfonamides target splicing by inducing RBM39 degradation via recruitment to DCAF15. Science 2017, 356, No. eaal3755.

(6) Uehara, T.; Minoshima, Y.; Sagane, K.; Sugi, N. H.; Mitsuhashi, K. O.; Yamamoto, N.; Kamiyama, H.; Takahashi, K.; Kotake, Y.; Uesugi, M.; Yokoi, A.; Inoue, A.; Yoshida, T.; Mabuchi, M.; Tanaka, A.; Owa, T. Selective degradation of splicing factor CAPERα by anticancer sulfonamides. Nat. Chem. Biol. 2017, 13, 675−680.

(7) Słabicki, M.; Kozicka, Z.; Petzold, G.; Li, Y. D.; Manojkumar, M.; Bunker, R. D.; Donovan, K. A.; Sievers, Q. L.; Koeppel, J.; Suchyta, D.; Sperling, A. S.; Fink, E. C.; Gasser, J. A.; Wang, L. R.; Corsello, S. M.; Sellar, R. S.; Jan, M.; Gillingham, D.; Scholl, C.; Fröhling, S.; Golub, T. R.; Fischer, E. S.; Thomä, N. H.; Ebert, B. L. The CDK inhibitor CR8 acts as a molecular glue degrader that depletes cyclin K. Nature 2020, 585, 293−297.

(8) Mayor-Ruiz, C.; Bauer, S.; Brand, M.; Kozicka, Z.; Siklos, M.; Imrichova, H.; Kaltheuner, I. H.; Hahn, E.; Seiler, K.; Koren, A.; Petzold, G.; Fellner, M.; Bock, C.; Müller, A. C.; Zuber, J.; Geyer, M.; Thomä, N. H.; Kubicek, S.; Winter, G. E. Rational discovery of molecular glue degraders via scalable chemical profiling. Nat. Chem. Biol. 2020, 16, 1199−1207.

(9) Lv, L.; Chen, P.; Cao, L.; Li, Y.; Zeng, Z.; Cui, Y.; Wu, Q.; Li, J.; Wang, J. H.; Dong, M. Q.; Qi, X.; Han, T. Discovery of a molecular glue promoting CDK12-DDB1 interaction to trigger cyclin K degradation. Elife 2020, 9, No. e59994.

(10) Krönke, J.; Fink, E. C.; Hollenbach, P. W.; MacBeth, K. J.; Hurst, S. N.; Udeshi, N. D.; Chamberlain, P. P.; Mani, D. R.; Man, H. W.; Gandhi, A. K.; Svinkina, T.; Schneider, R. K.; McConkey, M.; Järås, M.; Griffiths, E.; Wetzler, M.; Bullinger, L.; Cathers, B. E.; Carr, S. A.; Chopra, R.; Ebert, B. L. Lenalidomide induces ubiquitination and degradation of CK1α in del(5q) MDS. Nature 2015, 523, 183−188.

(11) Matyskiela, M. E.; Lu, G.; Ito, T.; Pagarigan, B.; Lu, C. C.; Miller, K.; Fang, W.; Wang, N. Y.; Nguyen, D.; Houston, J.; Carmel, G.; Tran, T.; Riley, M.; Nosaka, L.; Lander, G. C.; Gaidarova, S.; Xu, S.; Ruchelman, A. L.; Handa, H.; Carmichael, J.; Daniel, T. O.; Cathers, B. E.; Lopez-Girona, A.; Chamberlain, P. P. A novel cereblon modulator recruits GSPT1 to the CRL4(CRBN) ubiquitin ligase. Nature 2016, 535, 252−257.

(12) Donovan, K. A.; An, J.; Nowak, R. P.; Yuan, J. C.; Fink, E. C.; Berry, B. C.; Ebert, B. L.; Fischer, E. S. Thalidomide promotes degradation of SALL4, a transcription factor implicated in Duane Radial Ray syndrome. Elife 2018, 7, No. e38430.

(13) Asatsuma-Okumura, T.; Ando, H.; De Simone, M.; Yamamoto, J.; Sato, T.; Shimizu, N.; Asakawa, K.; Yamaguchi, Y.; Ito, T.; Guerrini, L.; Handa, H. p63 is a cereblon substrate involved in thalidomide teratogenicity. Nat. Chem. Biol. 2019, 15, 1077−1084.

(14) Yamamoto, J.; Suwa, T.; Murase, Y.; Tateno, S.; Mizutome, H.; Asatsuma-Okumura, T.; Shimizu, N.; Kishi, T.; Momose, S.; Kizaki, M.; Ito, T.; Yamaguchi, Y.; Handa, H. ARID2 is a pomalidomide-dependent CRL4(CRBN) substrate in multiple myeloma cells. Nat. Chem. Biol. 2020, 16, 1208−1217.

(15) Lai, A. C.; Crews, C. M. Induced protein degradation: an emerging drug discovery paradigm. Nat. Rev. Drug Discov. 2017, 16, 101−114.

(16) Schapira, M.; Calabrese, M. F.; Bullock, A. N.; Crews, C. M. Targeted protein degradation: expanding the toolbox. Nat. Rev. Drug Discov. 2019, 18, 949−963.

(17) Sun, X.; Gao, H.; Yang, Y.; He, M.; Wu, Y.; Song, Y.; Tong, Y.; Rao, Y. PROTACs: great opportunities for academia and industry. Signal Transduct. Target. Ther. 2019, 4, 64.

(18) Nalawansha, D. A.; Crews, C. M. PROTACs: an emerging therapeutic modality in precision medicine. Cell Chem. Biol. 2020, 27, 998−1014.

(19) Lu, J.; Qian, Y.; Altieri, M.; Dong, H.; Wang, J.; Raina, K.; Hines, J.; Winkler, J. D.; Crew, A. P.; Coleman, K.; Crews, C. M. Hijacking the E3 ubiquitin ligase cereblon to efficiently target BRD4. Chem. Biol. 2015, 22, 755−763.

(20) Winter, G. E.; Buckley, D. L.; Paulk, J.; Roberts, J. M.; Souza, A.; Dhe-Paganon, S.; Bradner, J. E. Phthalimide conjugation as a strategy for in vivo target protein degradation. Science 2015, 348, 1376−1381.

(21) Dale, B.; Cheng, M.; Park, K.-S.; Kaniskan, H. Ü.; Xiong, Y.; Jin, J. Advancing targeted protein degradation for cancer therapy. Nat. Rev. Cancer 2021 in press, DOI: 10.1038/s41568-021-00365-x.

(22) Mullard, A. Targeted protein degraders crowd into the clinic. Nat. Rev. Drug Discov. 2021, 20, 247−250.

(23) Rehman, W.; Arfons, L. M.; Lazarus, H. M. The rise, fall and subsequent triumph of thalidomide: lessons learned in drug development. Ther. Adv. Hematol. 2011, 2, 291−308.

(24) Ishoey, M.; Chorn, S.; Singh, N.; Jaeger, M. G.; Brand, M.; Paulk, J.; Bauer, S.; Erb, M. A.; Parapatics, K.; Müller, A. C.; Bennett, K. L.; Ecker, G. F.; Bradner, J. E.; Winter, G. E. Translation termination factor GSPT1 Is a phenotypically relevant off-target of heterobifunctional phthalimide degraders. ACS Chem. Biol. 2018, 13, 553−560.

(25) Pillow, T. H.; Adhikari, P.; Blake, R. A.; Chen, J.; Del Rosario, G.; Deshmukh, G.; Figueroa, I.; Gascoigne, K. E.; Kamath, A. V.; Kaufman, S.; Kleinheinz, T.; Kozak, K. R.; Latifi, B.; Leipold, D. D.; Sing Li, C.; Li, R.; Mulvihill, M. M.; O'Donohue, A.; Rowntree, R. K.; Sadowsky, J. D.; Wai, J.; Wang, X.; Wu, C.; Xu, Z.; Yao, H.; Yu, S. F.; Zhang, D.; Zang, R.; Zhang, H.; Zhou, H.; Zhu, X.; Dragovich, P. S. Antibody conjugation of a chimeric BET degrader enables in vivo activity. ChemMedChem 2020, 15, 17−25.

(26) Maneiro, M. A.; Forte, N.; Shchepinova, M. M.; Kounde, C. S.; Chudasama, V.; Baker, J. R.; Tate, E. W. Antibody-PROTAC conjugates enable HER2-dependent targeted protein degradation of BRD4. ACS Chem. Biol. 2020, 15, 1306−1312.

(27) Dragovich, P. S.; Pillow, T. H.; Blake, R. A.; Sadowsky, J. D.; Adaligil, E.; Adhikari, P.; Bhakta, S.; Blaquiere, N.; Chen, J.; dela Cruz-Chuh, J.; Gascoigne, K. E.; Hartman, S. J.; He, M.; Kaufman, S.; Kleinheinz, T.; Kozak, K. R.; Liu, L.; Liu, Q.; Liu, Q.; Lu, Y.; Meng, F.; Mulvihill, M. M.; O'Donohue, A.; Rowntree, R. K.; Staben, S. T.; Staben, S. T.; Wai, J.; Wang, J.; Wei, B. Q.; Wilson, C.; Xin, J.; Xu, Z.; Yao, H.; Zhang, H.; Zhang, H.; Zhou, H.; Zhu, X. Antibody-mediated delivery of chimeric BRD4 degraders. Part 1: exploration of antibody linker, payload loading, and payload molecular properties. *J. Med. Chem.* **2021**, *64*, 2534−2575.

(28) Dragovich, P. S.; Pillow, T. H.; Blake, R. A.; Sadowsky, J. D.; Adaligil, E.; Adhikari, P.; Chen, J.; Corr, N.; dela Cruz-Chuh, J.; del Rosario, G.; Fullerton, A.; Hartman, S. J.; Jiang, F.; Kaufman, S.; Kleinheinz, T.; Kozak, K. R.; Liu, L.; Lu, Y.; Mulvihill, M. M.; Murray, J. M.; O'Donohue, A.; Rowntree, R. K.; Sawyer, W. S.; Staben, L. R.; Wai, J.; Wang, J.; Wei, B.; Wei, W.; Xu, Z.; Yao, H.; Yu, S. F.; Zhang, D.; Zhang, H.; Zhang, S.; Zhao, Y.; Zhou, H.; Zhu, X. Antibody-mediated delivery of chimeric BRD4 degraders. Part 2: improvement of in vitro antiproliferation activity and in vivo antitumor efficacy. *J. Med. Chem.* **2021**, *64*, 2576−2607.

(29) Dragovich, P. S.; Adhikari, P.; Blake, R. A.; Blaquiere, N.; Chen, J.; Cheng, Y. X.; den Besten, W.; Han, J.; Hartman, S. J.; He, J.; He, M.; Rei Ingalla, E.; Kamath, A. V.; Kleinheinz, T.; Lai, T.; Leipold, D. D.; Li, C. S.; Liu, Q.; Lu, J.; Lu, Y.; Meng, F.; Meng, L.; Ng, C.; Peng, K.; Lewis Phillips, G.; Pillow, T. H.; Rowntree, R. K.; Sadowsky, J. D.; Sampath, D.; Staben, L.; Staben, S. T.; Wai, J.; Wan, K.; Wang, X.; Wei, B.; Wertz, I. E.; Xin, J.; Xu, K.; Yao, H.; Zang, R.; Zhang, D.; Zhou, H.; Zhao, Y. Antibody-mediated delivery of chimeric protein degraders which target estrogen receptor alpha (ERα). *Bioorg. Med. Chem. Lett.* **2020**, *30*, No. 126907.

(30) Scaranti, M.; Cojocaru, E.; Banerjee, S.; Banerji, U. Exploiting the folate receptor α in oncology. *Nat. Rev. Clin. Oncol.* **2020**, *17*, 349−359.

(31) Frigerio, B.; Bizzoni, C.; Jansen, G.; Leamon, C. P.; Peters, G. J.; Low, P. S.; Matherly, L. H.; Figini, M. Folate receptors and transporters: biological role and diagnostic/therapeutic targets in cancer and other diseases. *J. Exp. Clin. Cancer Res.* **2019**, *38*, 125.

(32) Zhou, Y.; Unno, K.; Hyjek, E.; Liu, H.; Zimmerman, T.; Karmakar, S.; Putt, K. S.; Shen, J.; Low, P. S.; Wickrema, A. Expression of functional folate receptors in multiple myeloma. *Leuk. Lymphoma* **2018**, *59*, 2982−2989.

(33) Zhu, W. Y.; Alliegro, M. A.; Melera, P. W. The rate of folate receptor alpha (FR alpha) synthesis in folate depleted CHL cells is regulated by a translational mechanism sensitive to media folate levels, while stable overexpression of its mRNA is mediated by gene amplification and an increase in transcript half-life. *J. Cell. Biochem.* **2001**, *81*, 205−219.

(34) Hsueh, C. T.; Dolnick, B. J. Altered folate-binding protein mRNA stability in KB cells grown in folate-deficient medium. *Biochem. Pharmacol.* **1993**, *45*, 2537−2545.

(35) Liu, J.; Chen, H.; Liu, Y.; Shen, Y.; Meng, F.; Kaniskan, H. Ü.; Jin, J.; Wei, W. Cancer selective target degradation by folate-caged PROTACs. *J. Am. Chem. Soc.* **2021**, *143*, 7380−7387.

(36) Fischer, E. S.; Böhm, K.; Lydeard, J. R.; Yang, H.; Stadler, M. B.; Cavadini, S.; Nagel, J.; Serluca, F.; Acker, V.; Lingaraju, G. M.; Tichkule, R. B.; Schebesta, M.; Forrester, W. C.; Schirle, M.; Hassiepen, U.; Ottl, J.; Hild, M.; Beckwith, R. E.; Harper, J. W.; Jenkins, J. L.; Thomä, N. H. Structure of the DDB1-CRBN E3 ubiquitin ligase in complex with thalidomide. *Nature* **2014**, *512*, 49−53.

(37) Liu, J.; Chen, H.; Ma, L.; He, Z.; Wang, D.; Liu, Y.; Lin, Q.; Zhang, T.; Gray, N.; Kaniskan, H. Ü.; Jin, J.; Wei, W. Light-induced control of protein destruction by opto-PROTAC. *Sci. Adv.* **2020**, *6*, No. eaay5154.

(38) Zhang, C.; Han, X. R.; Yang, X.; Jiang, B.; Liu, J.; Xiong, Y.; Jin, J. Proteolysis targeting chimeras (PROTACs) of anaplastic lymphoma kinase (ALK). *Eur. J. Med. Chem.* **2018**, *151*, 304−314.

(39) Zhang, H.; Wang, K.; Na, K.; Li, D.; Li, Z.; Zhao, D.; Zhong, L.; Wang, M.; Kou, L.; Luo, C.; Zhang, H.; Kan, Q.; Ding, H.; He, Z.;

Sun, J. Striking a balance between carbonate/carbamate linkage bond- and reduction-sensitive disulfide bond-bearing linker for tailored controlled release: in situ covalent-albumin-binding gemcitabine prodrugs promote bioavailability and tumor accumulation. *J. Med. Chem.* **2018**, *61*, 4904−4917.

(40) Santra, S.; Kaittanis, C.; Santiesteban, O. J.; Perez, J. M. Cell-specific, activatable, and theranostic prodrug for dual-targeted cancer imaging and therapy. *J. Am. Chem. Soc.* **2011**, *133*, 16680−16688.

(41) Ducry, L.; Stump, B. Antibody-drug conjugates: linking cytotoxic payloads to monoclonal antibodies. *Bioconjugate Chem.* **2010**, *21*, 5−13.

(42) Galzigna, L.; Rizzoli, V.; Schiappelli, P.; Moretto, C.; Bernareggi, A. S-acetyl- and S-phenylacetyl-glutathione as glutathione precursors in rat plasma and tissue preparations. *Enzyme Protein* **1994**, *48*, 98−104.

(43) Cacciatore, I.; Cornacchia, C.; Pinnen, F.; Mollica, A.; Di Stefano, A. Prodrug approach for increasing cellular glutathione levels. *Molecules* **2010**, *15*, 1242−1264.

(44) Subtil, A.; Gaidarov, I.; Kobylarz, K.; Lampson, M. A.; Keen, J. H.; McGraw, T. E. Acute cholesterol depletion inhibits clathrin-coated pit budding. *Proc. Natl. Acad. Sci. U. S. A.* **1999**, *96*, 6775−6780.

(45) Lee, D. H.; Goldberg, A. L. Proteasome inhibitors: valuable new tools for cell biologists. *Trends Cell Biol.* **1998**, *8*, 397−403.

(46) Soucy, T. A.; Smith, P. G.; Milhollen, M. A.; Berger, A. J.; Gavin, J. M.; Adhikari, S.; Brownell, J. E.; Burke, K. E.; Cardin, D. P.; Critchley, S.; Cullis, C. A.; Doucette, A.; Garnsey, J. J.; Gaulin, J. L.; Gershman, R. E.; Lublinsky, A. R.; McDonald, A.; Mizutani, H.; Narayanan, U.; Olhava, E. J.; Peluso, S.; Rezaei, M.; Sintchak, M. D.; Talreja, T.; Thomas, M. P.; Traore, T.; Vyskocil, S.; Weatherhead, G. S.; Yu, J.; Zhang, J.; Dick, L. R.; Claiborne, C. F.; Rolfe, M.; Bolen, J. B.; Langston, S. P. An inhibitor of NEDD8-activating enzyme as a new approach to treat cancer. *Nature* **2009**, *458*, 732−736.

(47) Bondeson, D. P.; Smith, B. E.; Burslem, G. M.; Buhimschi, A. D.; Hines, J.; Jaime-Figueroa, S.; Wang, J.; Hamman, B. D.; Ishchenko, A.; Crews, C. M. Lessons in PROTAC design from selective degradation with a promiscuous warhead. *Cell Chem. Biol.* **2018**, *25*, 78−87.e5.

(48) Morris, S.; Kirstein, M.; Valentine, M.; Dittmer, K.; Shapiro, D.; Saltman, D.; Look, A. Fusion of a kinase gene, ALK, to a nucleolar protein gene, NPM, in non-Hodgkin's lymphoma. *Science* **1994**, *263*, 1281−1284.

(49) Soda, M.; Choi, Y. L.; Enomoto, M.; Takada, S.; Yamashita, Y.; Ishikawa, S.; Fujiwara, S.; Watanabe, H.; Kurashina, K.; Hatanaka, H.; Bando, M.; Ohno, S.; Ishikawa, Y.; Aburatani, H.; Niki, T.; Sohara, Y.; Sugiyama, Y.; Mano, H. Identification of the transforming EML4-ALK fusion gene in non-small-cell lung cancer. *Nature* **2007**, *448*, 561−566.

(50) Tan, X.; Lu, X.; Jia, F.; Liu, X.; Sun, Y.; Logan, J. K.; Zhang, K. Blurring the role of oligonucleotides: spherical nucleic acids as a drug delivery vehicle. *J. Am. Chem. Soc.* **2016**, *138*, 10834−10837.

(51) Liu, J.; Peng, Y.; Shi, L.; Wan, L.; Inuzuka, H.; Long, J.; Guo, J.; Zhang, J.; Yuan, M.; Zhang, S.; Wang, X.; Gao, J.; Dai, X.; Furumoto, S.; Jia, L.; Pandolfi, P. P.; Asara, J. M.; Kaelin, W. G., Jr.; Liu, J.; Wei, W. Skp2 dictates cell cycle-dependent metabolic oscillation between glycolysis and TCA cycle. *Cell Res.* **2021**, *31*, 80−93.